Nanosensor detection of reactive oxygen and nitrogen species leakage in frustrated phagocytosis of nanofibres

Yu-Ting Qi, Fu-Li Zhang, Si-Yu Tian, Hui-Qian Wu, Yi Zhao, Xin-Wei Zhang, Yan-Ling Liu, Pingqing Fu, Christian Amatore, Wei-Hua Huang

Nanosensor Detection of Reactive Oxygen and Nitrogen Species Leakage in Frustrated Phagocytosis of Nanofibers

Yu-Ting Qi[1], Fu-Li Zhang[1], Si-Yu Tian[1], Hui-Qian Wu[1], Yi Zhao[1], Xin-Wei Zhang[1], Yan-Ling Liu[1], Pingqing Fu[5], Christian Amatore*[,3,4], and Wei-Hua Huang*[,1,2]

[1] College of Chemistry and Molecular Sciences, Wuhan University, Wuhan 430072, P. R. China

[2] Department of Hepatobiliary and Pancreatic Surgery, Zhongnan Hospital of Wuhan University, Wuhan 430071, P. R. China

[3] State Key Laboratory of Physical Chemistry of Solid Surfaces, College of Chemistry and Chemical Engineering, Xiamen University, Xiamen 361005, P. R. China

[4] PASTEUR, Département de Chimie, École Normale Supérieure, PSL Research University, Sorbonne University, UPMC Univ. Paris 06, CNRS 24 rue Lhomond, Paris 75005, France

[5] Institute of Surface-Earth System Science, School of Earth System Science, Tianjin University, Tianjin 300072, P. R. China

Abstract

Exposure to widely used inert fibrous nanomaterials (e.g., glass fibers, carbon nanotubes) might result in asbestos-like lung pathologies, becoming an important environmental and health concern. However, the origin of the pathogenesis of such fibers had not yet been clearly established. Here, we report on an electrochemical nanosensor which is used to monitor and quantitatively characterize the flux and dynamics of reactive species release during the progress of frustrated phagocytosis of glass nanofibers by single macrophages. We show the existence of an intense prolonged release of reactive oxygen and nitrogen species (ROS/RNS) by single macrophages at the level of their phagocytic cups. This continued massive ROS and RNS leakage damages peripheral cells and eventually translates into chronic inflammation and lung injury, as seen in in vitro co-culture and in vivo experiments.

Key Words: frustrated phagocytosis; glass fiber; nano-electrochemical sensor; ROS/RNS leakage; lung injury

Chemically inert fibrous nanomaterials are widely used in construction, textiles, medicine and many other fields. However, the application of such materials is associated with the inherent possibility of fiber release and public exposure.[1-4] Studies published over the past decades have proved that exposure to various nanofibers with widely different chemical compositions could cause diseases similar to those induced by asbestos, namely pulmonary inflammation and pulmonary fibrosis.[5-11] This suggested that the toxicity of these nanofibers was not only due to their surface chemical properties but mostly to their shapes and dimensions.

When small living or mineral exogenous entities enter the body, tissue-resident–macrophages quickly identify them and attempt to eliminate them by phagocytosis.[12-15] However, unlike pathogens that are easily engulfed and broken down into small molecules inside sealed phagolysosomes of macrophages, fibrous nanomaterials are too long to be fully taken up by macrophages and too stable to gradually degrade in pieces. This leads to a situation known as "frustrated phagocytosis",[6,8,9,13,16] which can last a long time depending on the length and chemical nature of the fiber. Reactive oxygen and nitrogen species (ROS/RNS) are therefore expected to be continuously produced by the concerted action of pools of NADPH oxidases (NOX) and inducible nitric oxide synthases (iNOS) active in the unsealed phagolysosome. Indeed, the resulting involvement of homeostatic behaviors[17] is expected to cause a sustained release of ROS/RNS leaking out of the macrophages' cups.[18-20] If this scenario did indeed occur, such continued blasting of surrounding lung tissue by ROS/RNS is expected to lead to peripheral cells damage and local chronic inflammation that could eventually develop into diseases such as lung fibrosis and lung cancer.[13,16]

Over the past decades, several investigations involving ROS/RNS staining or extended in vivo experiments performed with fibrous nanomaterials, including carbon nanotubes and asbestos, have supported this hypothesis.[16,21,22] However, neither the chemical nature of the leaking reactive species nor the spatio-temporal characteristics of their distributions could be revealed due to the lack of suitable precise analytical sensors.

Conversely, new generations of nano-electrochemical bio-sensors allow highly sensitive and accurate measurements with high selectivity and excellent spatiotemporal resolution, thus enabling the characterization and quantification of molecular fluxes at single cells or at the organelles level inside living cells without damaging their integrity and functionalities.[19,23-26] Besides, many works have established the Pt-black electrode unique capability for individually monitoring the concentrations of the four primary ROS/RNS ($ONOO^-$, H_2O_2, NO and NO_2^-) and tracking their time variations with adjustable spatiotemporal.[17,19,27-34]

Our previous Pt-black decorated SiC nanowires electrochemical sensors (SiC@Pt NW) were selected to monitor the intensities and temporal variations of ROS/RNS fluxes emitted by single macrophages undergoing frustrated glass nanofibers phagocytosis (Fig. 1a). This allowed to demonstrate for the first time that ROS/RNS were massively released through the unsealed phagocytic cups and, interestingly, that their fluxes continuously increased until the glass nanofibers could be completely encapsulated. These sustained, intense and localized releases of ROS/RNS exposed adjacent cells to severe oxidative stress conditions. Under in vivo conditions, this led to chronic inflammation in lung tissue following continuous local damages, as demonstrated by cell co-culture and in vivo experiments.

Frustrated Phagocytosis of Glass Fibers into Macrophages

All glass nanofibers extracted from quartz filter membranes exhibited regular cylindrical shapes with an average diameter of 650 nm. They were separated into two classes by filtration through meshes of different pore sizes (Extended Data Fig. 1a-c): the "long" ones had an average length of 70 µm, while the "short" ones had an average length of 10 µm. The fibers of each class were essentially composed of Si and O elements (Extended Data Fig. 1d-e) without any endotoxin contamination (Extended Data Fig. 1f). When RAW 264.7 murine macrophages were preincubated in the presence of long or short glass nanofibers, they underwent frustrated phagocytosis (Fig. 1) but maintained their high viability (80% for long fibers and 94% for short fibers) as evidenced by fluorescent staining, as well as the release of lactate dehydrogenase (LDH) (Extended Data Fig. 2a-b).Consistent with previous reports, the morphology of the resting-type macrophages (M0) underwent significant changes with an evident extension of cell bodies along the fibers axes to eventually adopt stretched and polarized shapes (M1-like macrophage with high expression of iNOS and CD86) around the glass nanofibers axes[9,35,36] (supplementary bright-field videos 1-2, confocal videos 1-2 and Extended Data Fig. 2c-d). Besides, phalloidin-labelled actin exhibited initially the circular cell outlines of M0 macrophages evolved into spindle-like shapes after 12 h of continuously frustrated phagocytosis (Fig. 1b) Importantly, clearly visible actin rings appeared at the poles of the active polarized macrophages at the very place where they connected to the still unengaged parts of the glass nanofibers, suggesting the formation of phagocytic cups[37-39] (Fig. 1b, white arrowheads in the right photo). Confocal 3D images proved that the captured fractions of nanofibers were indeed internalized by macrophages rather than remaining stuck to their membrane surface or lying under the cells (Fig. 1c and Extended Data Fig. 2e). Transmission electron microscopy (TEM) confirmed the partial internalization of glass nanofibers by these cells; by comparison, M0 cells evidenced their near spherical clear cytoplasm (Fig. 1d). Altogether, these experiments perfectly revealed that even after a long 12 h duration, the macrophages could not completely engulf the glass nanofibers and displayed all characteristics of "frustrated phagocytosis". This suggested that ROS/RNS could continuously spill over onto the adjacent tissue from the macrophages' unsealed phagocytic cups.

Quantitative ROS/RNS Spillover During Frustrated Phagocytosis

To study the intensities and chemical nature of ROS/RNS fluxes emitted by macrophages, the tip of SiC@Pt NW sensor was positioned at specific locations on their bodies surfaces and at different stages (0, 4, 12, 20 and 24 h) of their frustrated phagocytosis of glass nanofibers (as sketched in Fig. 1a on the right). Moreover, the time-dependent production rates of each primary ROS/RNS species, $f_{species}(t)$, could be obtained quantitatively with quadruple potential chronoamperometric sequences (Extended Data Fig. 3).[19,29,33]

Upon positioning the tip of SiC@Pt NW sensor on the top of M0 cells, the oxidative currents increased slightly before gradually decreasing to their basal levels, providing evidence that the macrophage was sensitive to the mechanical strain imposed by the nanosensor tip and responded quickly by releasing small amounts of ROS/RNS (Extended Data Fig. 4a-b). According to equations (1-4) (Methods section) the production rates of four primary ROS/RNS (Extended Data Fig. 4c) from which those of their two precursors $O_2^{\bullet-}$ and NO

(Extended Data Fig. 4d) were deduced according to the reaction stoichiometries reported in Extended Data Fig. 3d. Extended Data Fig. 4e compares these relative productions during the first 40 min (see statistical data in Supplementary Table 1). This evidenced that the total production of the parent superoxide ions was ca. 2.5 times that of the parent NO, which is in agreement with an immune mechanism involving a fast ROS production at an early stage of pathogen clearance,[40] and a NO production by iNOS being mainly regulated at the transcriptional level,[40-42] as confirmed by immunofluorescence staining (Extended Data Fig. 5a-b). NOX which is well expressed in the resting state compared to iNOS provided ca. 70% of total reactive species, allowing a rapid response of macrophages to the mechanical stimulation by the nanosensor tip pressure.

After 4 h of attempted phagocytosis, macrophages enveloped part of the glass nanofibers by gradually extending their pseudopodia upwards to capture the fibers without displaying other noticeable morphological changes (Fig. 2a and first row of Extended Data Fig. 2f) , which is consistent with Padmore et al.'s findings.[8]. As soon as the SiC@Pt NW sensor tip was positioned close to a cell/nanofiber junction point (see Fig. 2a and photograph in Fig. 2b inset), the current increased significantly compared with distal outer regions, evidencing that the progress of the immune responses involved a significant localized leakage of ROS/RNS during the attempted phagocytosis (Fig. 2b). Analysis of the corresponding current traces allowed identifying and quantifying the release rates of each of the four primary ROS/RNS (Fig. 2c), from which their two precursors, $O_2^{\bullet-}$ and NO, production rates could be extracted (Fig. 2d). Statistical analyses (6 macrophages) confirmed these results as evidenced by the magnitude of their fluxes released near their phagocytotic cups: $f_{ONOO^-} = 1.3 \pm 0.3\ amol/s$, $f_{H_2O_2} = 4.1 \pm 0.4\ amol/s$, $f_{NO} = 4.9 \pm 0.7\ amol/s$, and $f_{NO_2^-} = 1.2 \pm 0.3\ amol/s$, corresponding to $f_{O_2^{\bullet-}}^{parent} = 10.6 \pm 0.8\ amol/s$ and $f_{NO}^{parent} = 7.5 \pm 0.8\ amol/s$ for the $O_2^{\bullet-}$ and NO precursors (Fig. 2e). Interestingly, the overall parent NO production increased by ca. 1/3 compared to what was observed for the M0 type (Fig. 2d), indicating an enhanced iNOS expression in agreement with immunofluorescence imaging (Extended Data Fig. 5a-b).

After 12 h phagocytosis, the cells morphologies were drastically altered with cell bodies elongating along the fiber axis to exhibit a spindle shape (Fig. 3a and second row of Extended Data Fig. 2f). To investigate the spatial distribution of ROS/RNS emissions from these fully polarized cells, the SiC@Pt NW sensor tip (poised at +800 mV vs. Ag/AgCl to monitor all ROS/RNS together) was scanned along the cell membrane and the partially engulfed nanofiber (Extended Data Fig. 5c) to determine local intensities of ROS/RNS emissions and identify major leak sites if any. This revealed very marked spatial differences in ROS/RNS release amounts with the highest ones leaking from the phagocytic cups areas while the smallest ones coming from the top of the cell (Extended Data Fig. 5d).

In order to analyze the relative production of each primary ROS/RNS and average them over a meaningful duration (2 h), the nanosensor tip was located at the level of the phagocytic cup of a cell having partially engulfed a glass nanofiber (Fig. 3a) or at its top and subjected to the staircase potential sequence described above (Extended Data Fig. 3b). The recorded currents (Fig. 3b-c) confirmed the occurrence of a greater ROS/RNS leakage at the phagocytic cups, being more than three times that at the top of the cell, and demonstrated that the composition of the ROS/RNS cocktail also significantly depended of the location of the

tip (Fig. 3d-e and Fig. 3g-h). Statistical analyses (6 macrophages) confirmed the data in Fig. 3b-c. Indeed, at the phagocytotic cups (Fig. 3f) one obtained $f_{ONOO^-} = 1.9 \pm 0.1\ amol/s$, $f_{H_2O_2} = 8.7 \pm 0.5\ amol/s$, $f_{NO} = 29.5 \pm 1.2\ amol/s$, and $f_{NO_2^-} = 4.7 \pm 0.3\ amol/s$, corresponding to $f_{O_2^{\cdot-}}^{parent} = 24.0 \pm 0.9\ amol/s$ and $f_{NO}^{parent} = 36.2 \pm 0.9\ amol/s$ for $O_2^{\bullet-}$ and NO their precursors production rates. On the other side, at the top of cell (Fig. 3i) much modest values were found: $f_{ONOO^-} = 0.9 \pm 0.1\ amol/s$, $f_{H_2O_2} = 2.9 \pm 0.4\ amol/s$, $f_{NO} = 8.3 \pm 1.1\ amol/s$, and $f_{NO_2^-} = 1.2 \pm 0.3\ amol/s$, corresponding to production rates of their $O_2^{\bullet-}$ and NO precursors $f_{O_2^{\cdot-}}^{parent} = 7.9 \pm 0.6\ amol/s$ and $f_{NO}^{parent} = 10.4 \pm 0.9\ amol/s$.

These data demonstrated that after 12 h of frustrated phagocytosis large amounts of ROS/RNS were leaking from the phagocytic cup(s), with NO being now the major parent precursor (60%) vs. $O_2^{\bullet-}$ (40%). Such inversion in the proportions of ROS/RNS precursor productions relative to the early stages of attempted phagocytosis (dominated by $O_2^{\bullet-}$, see above) was consistent with reported stages of innate immune responses against fully engulfed pathogens.[17,40,43]

After 20 h of frustrated phagocytosis, cells achieved extremely stretched shapes and only a small portion of nanofibers remained exposed outside the cell while pseudopodia extended from the closed phagocytotic pocket end (Fig. 4a and third row of Extended Data Fig. 2f). The monitored currents increased sharply when the nanosensor tip was moved towards the phagocytic cup (Extended Data Fig. 6a-b) while exhibiting strong and infrequent peaks (Extended Data Fig. 6c-e) suggesting the occurrence of sudden events, such as extracellular secretion of lysosomes and late endosomes.[27,29] Statistical analysis (n = 6 macrophages analyzed over 1.5 h each) confirmed that the observation in Extended Data Fig. 6b was general by highlighting the leakage of considerable amounts of each ROS/RNS compared to earlier stages of frustrated phagocytosis: $f_{ONOO^-} = 7.2 \pm 0.4\ amol/s$, $f_{H_2O_2} = 29.6 \pm 1.6\ amol/s$, $f_{NO} = 102.4 \pm 5.4\ amol/s$, and $f_{NO_2^-} = 17.7 \pm 1.5\ amol/s$ (Fig. 4b). The productions of the initial precursors $O_2^{\bullet-}$ and NO were ca. four times larger than those measured after 12 h of frustrated phagocytosis: $f_{O_2^{\cdot-}}^{parent} = 84.1 \pm 2.6\ amol/s$ and $f_{NO}^{parent} = 127.3 \pm 5.7\ amol/s$ (Fig. 4b). Conversely, the amounts of ROS/RNS detected above the top of the cells remained low, being close to their previous levels, and without giving rise to strong sudden current peaks (Extended Data Fig. 6f-h): $f_{ONOO^-} = 1.0 \pm 0.1\ amol/s$, $f_{H_2O_2} = 3.7 \pm 0.5\ amol/s$, $f_{NO} = 11.0 \pm 1.8\ amol/s$ and $f_{NO_2^-} = 1.9 \pm 0.40\ amol/s$, corresponding to the initial precursors $O_2^{\bullet-}$ and NO production rates $f_{O_2^{\cdot-}}^{parent} = 10.3 \pm 0.9\ amol/s$ and $f_{NO}^{parent} = 13.9 \pm 1.6\ amol/s$ (Fig. 4c). These results clearly established that in response to difficult phagocytic situations, macrophages may strongly increase their production of ROS/RNS inside their phagocytic pockets, most of which leaks through the unsealed phagocytic cups, so without endangering their own bodies.[30]

After 24 h of unsuccessful phagocytosis, microphotographic images suggested that the cells could completely envelop the fibers by closing their phagocytic cups possibly through multicellular co-phagocytosis or self-division (Fig. 4d and fourth row of Extended Data Fig. 2f), which is reminiscent of granuloma, in which immune cells respond to a chronic inflammatory situation by isolating foreign substances that they are

unable to eliminate.[9-11](hebing)This was confirmed by monitoring the ROS/RNS fluxes released at the cells extremities with the SiC@Pt NW electrochemical sensors. These were significantly diminished, ca. by a factor 20 (Fig. 4e, Extended Data Fig. 7a-e, and Supplementary Table 1) compared to the observations made after 20 h of frustrated phagocytosis. The ROS/RNS fluxes recorded at the top of the cell were also much lower (Fig. 4f, Extended Data Fig. 7f-h and Supplementary Table 1). These results revealed that under our conditions, the attempted phagocytotic events ended in isolation of resistant nanofibers inside the cell envelope associated with a dramatic decrease in released ROS/RNS.

Short fibers and classical lipopolysaccharide (LPS) stimulation were used as control experiments to investigate the release of ROS/RNS. The magnitude of ROS/RNS release from macrophages that rapidly internalized short fibers (within 12 h) or after LPS stimulation was ca. 1/160 (Extended Data Fig. 8, Supplementary Table 2 and Fig. 5a-b) and ca. 1/80 (Extended Data Fig. 9a-d and Supplementary Table 3) respectively of that measured at the phagocytic cups after 20 h of frustrated phagocytosis long fibers. These results demonstrated that only frustrated phagocytosis triggered by long nanofibers could lead to intense ROS/RNS leakage prone to induce lesions of the tissues on which the fibers and macrophage rest.

Quantitative and Dynamic Variations of ROS/RNS Leakage

The above investigations established that the release of each primary ROS/RNS near the phagocytic cups differed significantly throughout the duration of frustrated phagocytosis, exhibiting a continuous increase during its early stages until reaching a peak at ca. 20 h followed by a drastic decline (lines in Fig. 5a), reflecting similar overall kinetics for the production of their precursors $O_2^{\bullet-}$ and NO (lines in Fig. 5b). The positional effect of ROS/RNS source, i.e., the ratio of the production rates at the cup/extremity to those at the cell top (f_{cup}/f_{top}), displayed a continuous increase, peaked at a value larger than 7 at 20 h and dramatically decreased at 24 h once the fibers were completely phagocytosed (Extended Data Fig. 9e-f). However, the relative proportions of the released ROS/RNS and of their precursors changed as the phagocytosis attempt progressed, with an early response (i.e., during the initial 4 hours) mostly involving NOX, viz., producing mainly $O_2^{\bullet-}$, while NO was later produced in larger amounts than $O_2^{\bullet-}$ showing the predominance of iNOS during the following stages (Fig. 5b-c). Besides, the response of short fibers exhibited the same homeostatic regulation of enzymes (Extended Data Fig. 8l-m and dotted lines in Fig. 5a-b). To our knowledge, these results established for the first time and on a quantitative basis essential characteristics of macrophages activities during their unsuccessful attempts to eliminate high aspect ratio nanomaterials resistant to ROS/RNS (Fig. 5d).

Once macrophages detect the glass nanofibers, they activate NOX and iNOS for the purpose of digesting the partially encapsulated nanofibers (Fig.5d, second cartoon on left side), thus causing an extensive leakage of ROS/RNS out the phagocytic cups in an attempt to maintain their homeostasis.[33,34] This intense leakage increases over nearly one day until the macrophages manage to alter their own aspect ratios to fully internalize the nanofibers possibly by recruiting surrounding cells to form multicellular co-phagosomes (Fig. 5d right cartoon). Moreover, large amounts of inflammatory cytokines were produced by glass nanofibers-stimulation. Consistent with the findings of Padmore et al.,[8] the production of tumor necrosis factor α (TNF-α), interleukin-

1 α (IL-1α), prostaglandin E2 (PGE-2) was 1.3, 2, and 1.7 times higher than that of the short fibers, respectively (Extended Data Fig. 9g). Massive released ROS/RNS could promote cytokine production, and these inflammatory cytokines in turn form a synergistic feedback loop with ROS/RNS, exacerbating the inflammatory response.[44]

However, before that may happen, if actual in vivo situations paralleled those monitored in this work, the surrounding tissues on which the nanofibers settled would have been subjected to intense and prolonged destructive fluxes of ROS/RNS and inflammatory factors, thus suffering severe damages.

Epithelial Cell Damages and Pulmonary Fibrosis

A model was carried out under in vitro conditions involving co-cultures of RAW 264.7 murine macrophages with murine MLE-12 lung epithelial cells seeded with glass nanofibers (see Fig. 6a, Extended Data Fig. 10a).

In the control co-culture group (i.e., with no exposure of macrophages to glass nanofibers), MLE-12 cells exhibited a spreading spindle shape and high viability. Conversely, in the co-culture test group, after 24 hours of exposure of macrophages to glass nanofibers, 15% of MLE-12 cells were dead, aggregated and exhibited a round shape (Fig. 6a), while exposure to soluble fractions of fibers in the absence of macrophages did not affect the cell viability (Extended Data Fig. 10a-b). These results fully validated our above hypothesis that intense ROS/RNS fluxes released by macrophages attempting to phagocytose glass nanofibers during lengthy time durations led to severe damage to co-cultured lung epithelial cells even when these cells were not in direct contact with the nanofibers.

To test the validity of these in vitro results in a more realistic situation, Sprague-Dawley (SD) rats were exposed to PBS-containing suspended glass nanofibers (0.5 mg/rat and 2 mg/rat) by intratracheal instillation. After 1, 3, 7 and 14 days, alveolar macrophages and lung tissue were collected for fluorescent staining and histopathology (Fig. 6b). The presence of single alveolar macrophages in the recovered bronchoalveolar lavage fluid was confirmed by immunofluorescence staining by Siglec F monoclonal antibody (Extended Data Fig. 10c);[45] flow cytometry results evidenced an increase in M1-like cells displaying higher expression of CD86 and CD80 in the fiber-stimulated group compared to that of the control group (Extended Data Fig. 10d). Glass nanofibers already taken up by single macrophages or multiple macrophages could be clearly observed (Fig. 6c and e) confirming the in vivo occurrence of frustrated phagocytosis and co-phagocytosis of glass nanofibers by macrophages. Additionally, the corresponding intense ROS/RNS spillage was confirmed by the high fluorescence intensities of ROS and NO (Fig. 6c-f).

As evidenced by hematoxylin and eosin (H&E) staining, glass nanofibers led to infiltration of inflammatory cells and thickening of the respiratory duct walls (Fig. 6g). After prolonged exposure time, Masson's trichrome staining confirmed the increase of collagen deposition in lung section (Fig. 6h), indicating worsening fibrotic lesions.[9-11,46] Furthermore, exposure to high dose (2 mg/rat) of glass nanofibers resulted in severe lesions, as evidenced by the identification of nanofibers within the alveoli with a non-uniform grainy appearance and increased collagen deposition (Extended Data Fig. 10e-h).

Conclusions

The existence and the spatiotemporal characteristics of intense continuous ROS/RNS leakage from single macrophages undergoing frustrated phagocytosis of high aspect ratio glass nanofibers was definitely proven, characterized and quantitatively monitored for the first time with the current SiC@Pt nanowire electrochemical sensors. Changes in chemical composition and kinetic variability of the massive ROS/RNS fluxes emitted through the unsealed phagocytotic cups involved a drastic inversion of the relative activities of NOX and iNOS with time over the one-day period. Such prolonged and massive ROS/RNS leakage resulted in severe damage to peripheral cells that eventually translated into chronic inflammation and lung injury, as could be evidenced and characterized by in vitro co-culture experiments and confirmed at the in vivo level.

The highly sensitive electrochemical nano-sensing approach reported in this work quantitatively and kinetically proved and supported previous hypotheses that lung injury associated with inhalation of chemically inert nanofibers occurs due to the action of prolonged massive fluxes of ROS/RNS emitted by macrophages undergoing frustrated phagocytosis of high aspect ratio inert nanomaterials.

Figure legends/captions (for main text figures)

Fig. 1 | Characterization of frustrated phagocytosis of glass fibers by macrophages. a) Schematic diagram describing the different stages of the frustrated phagocytosis of a glass nanofiber by a macrophage and the use of a SiC@Pt NW sensor for differentiating ROS/RNS released at different loci of the macrophage surface and quantifying their fluxes. **b)** Morphology of macrophages stained with phalloidin (orange) and Hoechst (blue) before (M0 state) and 12 h after beginning of frustrated phagocytosis (polarized state) of glass nanofibers (green). The highlighted orange areas pointed by the white arrowheads represent the actin rings present at the phagocytic cups. Scale bar, 10 µm. **c)** Z-stacked confocal image of macrophages 12 h after beginning of frustrated phagocytosis of glass nanofibers (see Extended Data Fig. 2e for the individual stacked Z-images). **d)** Transmission electron microscopy (TEM) of macrophages before (M0 state, left view) and after (polarized state, middle view) 12 h of frustrated phagocytosis of two glass nanofibers (shown by yellow arrows); the right TEM image shows more precisely one glass nanofiber (back area marked by yellow asterisk) encapsulated inside a phagolysosome (enlargement of zone marked by the yellow lines in middle view). Scale bars, 1 µm (left and middle), and 500 nm (right).

Fig. 2 | ROS/RNS production after 4 h of phagocytosis. a) Pseudo-color SEM images of macrophage (red) after 4 h of frustrated phagocytosis of a glass nanofiber (blue). Enlarged SEM images (right) showing details of the phagocytic zones marked by white dashed lines. Scale bars, 2 µm (left) and 500 nm (right). **b)** Time variations of the chronoamperometric currents measured at the end of each staircase period (i.e., every 80 s, see Extended Data Fig. 3a-c) at each stepped potential value: 150 (blue), 550 (gray), 650 (yellow), and 800 mV (green) vs. Ag/AgCl when the SiC@Pt NW sensor tip was positioned near one cell/nanofiber junction point (see panel c and photograph in inset; scale bar, 20 µm) at the moment indicated by the gray vertical arrow; the dashed line represents the chronoamperometric currents (baseline) at 150 mV for untreated (M0) macrophages (see details in Extended Data Fig. 4b). **c)** Corresponding time variations of $ONOO^-$ (blue), H_2O_2 (orange), NO (green), and NO_2^- (purple) production rates deduced from the currents in panel d by solving the system of equations (1-4) in Method section. **d)** Reconstructed time variations of the production rates of the two precursors $O_2^{\bullet-}$ (red) and NO (dark blue) based on the data in panel c according to the stoichiometries reported in Extended Data Fig. 3d. **e)** Statistical analyses (n= 6 macrophages) of the production rates of the four primary ROS/RNS and their precursors $O_2^{\bullet-}$ and NO within 1.5 h (means ± SEM; one-way ANOVA).

Fig. 3 | ROS/RNS production after 12 h of phagocytosis. **a)** Pseudo-color SEM image of macrophage (red) phagocytosis of glass nanofibers (blue) after 12 h of frustrated phagocytosis; scale bar, 5 µm. **b, c)** Time variations of the chronoamperometric currents measured at the phagocytic cup (**b**) and the cell top (**c**) as a function of the electrode potential values: 150 (blue), 550 (gray), 650 (yellow), and 800 mV (green) vs. Ag/AgCl; the gray vertical arrows indicate the moment when the SiC@Pt NW sensor tip was positioned close to the phagocytic cup or the cell top; insets: microphotographs of the NW sensors positioned at the phagocytic cup or the cell top; scale bars, 10 µm. **d, g)** Corresponding time variations of $ONOO^-$ (blue), H_2O_2 (orange), NO (green), and NO_2^- (purple) production rates at the phagocytic cup (**d**) and the cell top (**g**) as deduced from the currents in panels b and c, respectively. **e, h)** Time variations of the production rates of the two precursors $O_2^{\bullet-}$ (red) and NO (dark blue) at the phagocytic cup (**e**) and the cell top (**h**), as deduced from the data in panels d and g, respectively, according to the reactions stoichiometries reported in Extended Data Fig. 3d caption; the gray vertical arrows indicate the moment when the SiC@Pt NW sensor tip was positioned close to the phagocytic cup or on the cell top. **f, i)** Statistical analyses (n=6 macrophages) of the production rates over 1.5 h of four primary ROS/RNS and of their precursors $O_2^{\bullet-}$ and NO at the phagocytic cup (**f**) and the cell top (**i**) (means ± SEM; one-way ANOVA).

Fig. 4 | ROS/RNS production after 24 h of phagocytosis. a, d) Pseudo-color SEM images of macrophage (red) phagocytosis of glass nanofiber (blue) after 20 h (**a**) or 24 h (**d**) of frustrated phagocytosis**;** scale bars: 5 µm (main images), 1 µm (**a**, insets), and 500 nm (**d**, insets). **b, c, e, f)** Statistical analyses (n = 6 macrophages analyzed over 1.5 h each) of the production rates of

four primary ROS/RNS and of their precursors $O_2^{\bullet-}$ and NO at the phagocytic cup (**b**) and cell top (**c**) after 20 h (**b, c**) or 24 h (**e, f**) of attempted phagocytosis (means ± SEM; one-way ANOVA).

Fig. 5 | Dynamic variations of ROS/RNS leakage during frustrated phagocytosis. a, b) Time variation of the production rates of the four primary ROS/RNS (blue, $ONOO^-$; orange, H_2O_2; green, NO; and purple, NO_2^-) (**a**) and of their two precursors $O_2^{\bullet-}$ (red) and NO (dark blue) (**b**) released near a macrophage phagocytic cup during frustrated phagocytosis of a long (line) and short glass (dotted line) nanofiber. **c)** Same data as in panels a and b presented in terms of relative time-dependent proportions for the four primary ROS/RNS and their two precursors. **d)** Graphical summary of changes in ROS/RNS generation during attempted phagocytosis of glass nanofibers by macrophages; the relative diameters of colored spots around each of the four primary ROS/RNS represent their relative amounts detected while the thicknesses of arrows attached to each enzymatic pool represent their relative kinetic contributions.

Fig. 6 | Pulmonary injury induced by frustrated phagocytosis. a) Left: principle of the co-culture assay; right: calcein-AM and PI fluorescent staining of MLE-12 cells with (bottom) or without (top) RAW 264.7 cells exposure to glass nanofibers; yellow contours delineate clusters of aggregated cells; scale bar, 100 μm. **b)** Time-chart of the in vivo experiments. **c, e)** Bright-field and fluorescence microphotographs of alveolar macrophages stained with DC-FHDA (ROS probe) (**c**) or DAF-FM DA (NO probe) (**e**) and Hoechst, with magnified images of single macrophages undergoing phagocytosis (yellow arrowheads) or co-phagocytosis (red arrowheads) of long glass nanofibers shown on the side; scale bars, 50 μm and 10 μm (magnified views). **d, f)** Statistical analysis (n=90 macrophages from 3 rats) of the fluorescent intensity of DCFH-DA (**d**) and DAF-FM DA (**f**) (means ± SEM; one-way ANOVA). **g)** Representative hematoxylin and eosin (H&E) staining of lung sections with and without intratracheal glass nanofibers instillation for 14 days; alveolar macrophages pointed by the red arrows in the magnified image; scale bars, 100 μm (left), 20 μm (right). **h)** Masson's trichrome staining of lung sections with (bottom) and without (top) intratracheal glass nanofibers instillation; scale bar, 200 μm.

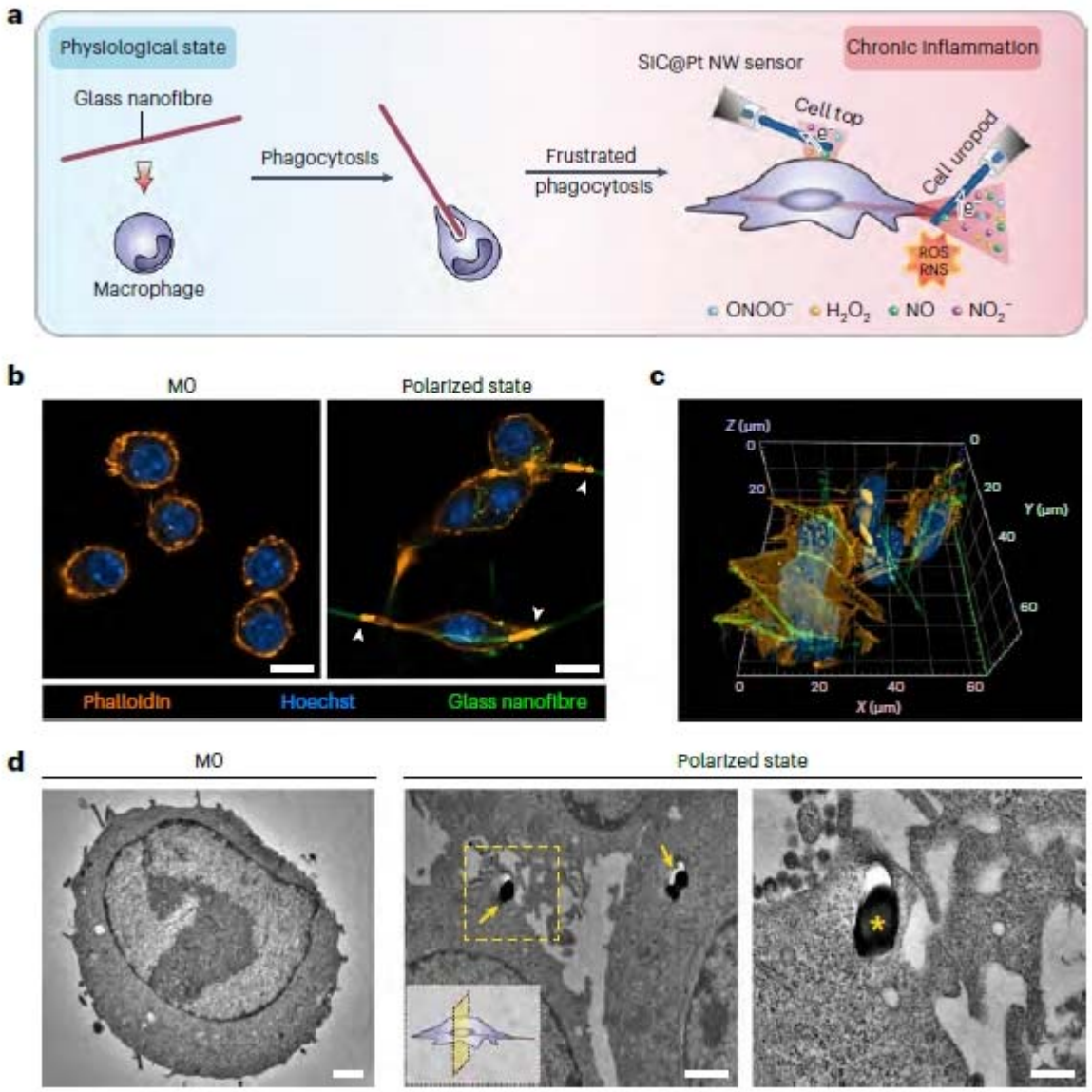
a
Physiological state
Glass nanofibre
Macrophage
Phagocytosis
Frustrated phagocytosis
SiC@Pt NW sensor
Chronic inflammation
Cell top
Cell uropod
ROS RNS
ONOO⁻ H2O2 NO NO2⁻
b
M0
Polarized state
Phalloidin
Hoechst
Glass nanofibre
c
Z (µm)
Y (µm)
X (µm)
d
M0
Polarized state

Fig 1

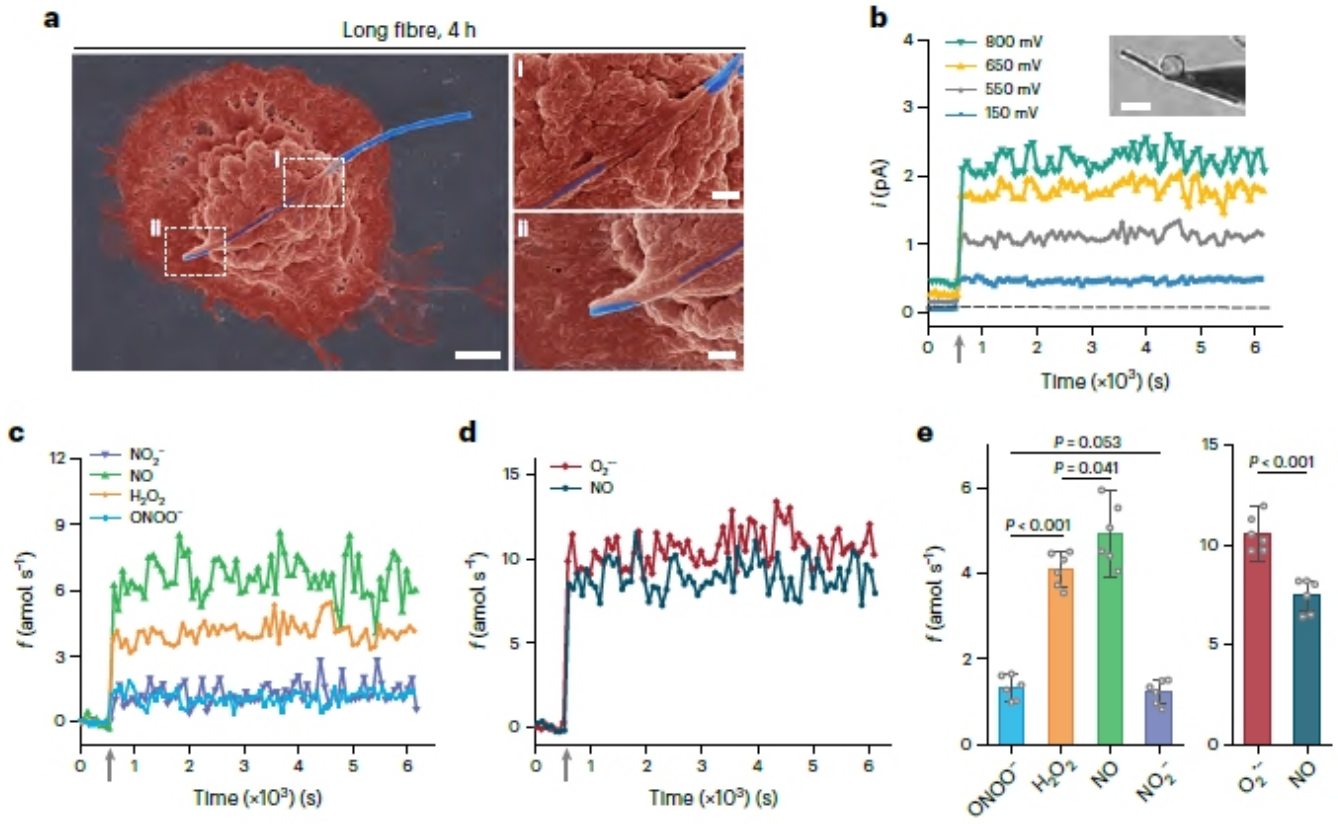
a
Long fibre, 4 h
I
II
i
ii
b
800 mV
650 mV
550 mV
150 mV
i (pA)
Time (×10³) (s)
c
NO₂⁻
NO
H₂O₂
ONOO⁻
f (amol s⁻¹)
Time (×10³) (s)
d
O₂⁻
NO
f (amol s⁻¹)
Time (×10³) (s)
e
P = 0.053
P = 0.041
P < 0.001
P < 0.001
f (amol s⁻¹)
ONOO⁻
H₂O₂
NO
NO₂⁻
O₂⁻
NO

Fig 2

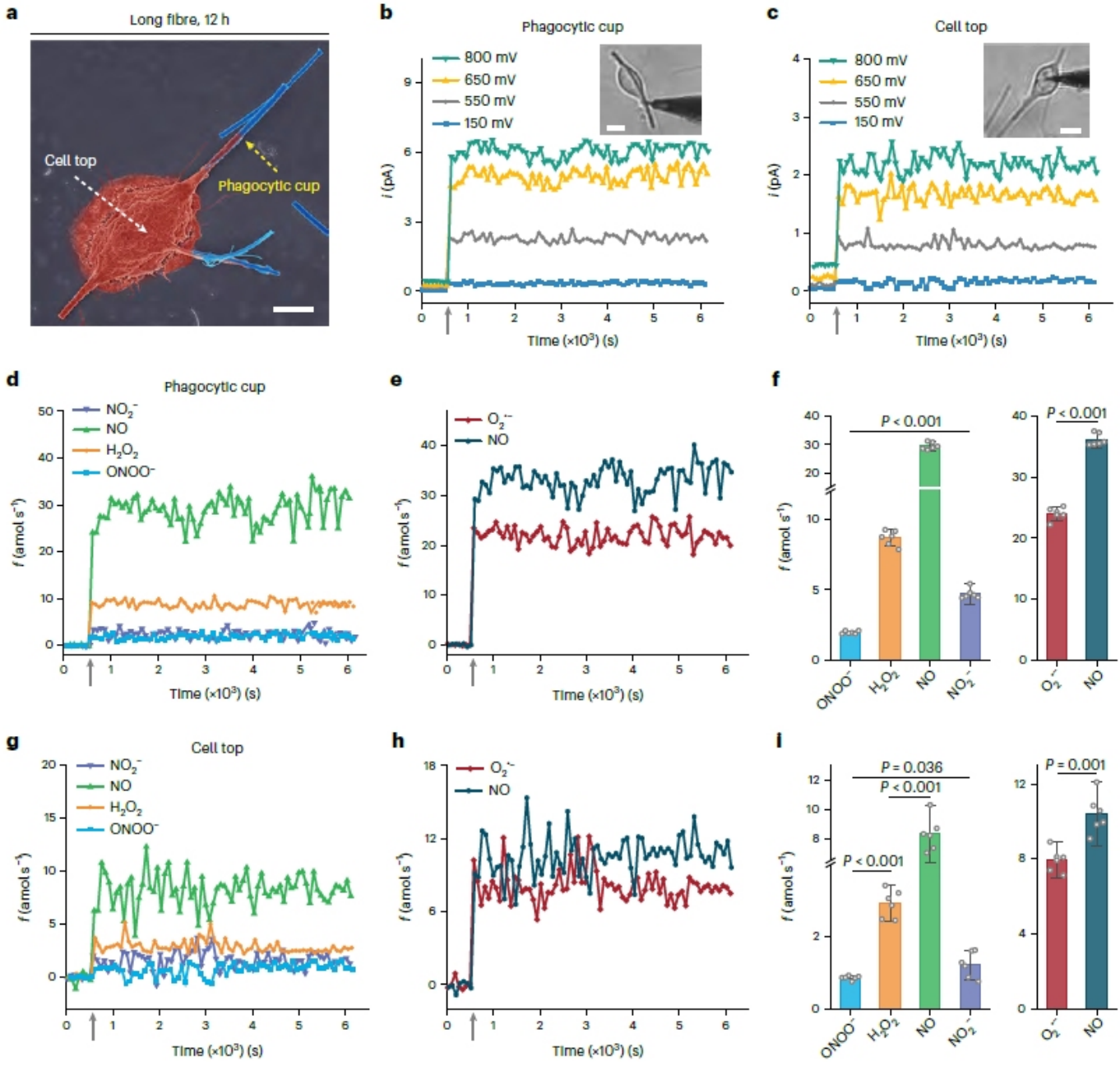
a
Long fibre, 12 h
Cell top
Phagocytic cup
b
Phagocytic cup
800 mV
650 mV
550 mV
150 mV
i (pA)
Time (×10³) (s)
c
Cell top
800 mV
650 mV
550 mV
150 mV
i (pA)
Time (×10³) (s)
d
Phagocytic cup
NO2−
NO
H2O2
ONOO−
f (amol s−1)
Time (×10³) (s)
e
O2•−
NO
f (amol s−1)
Time (×10³) (s)
f
P < 0.001
P < 0.001
f (amol s−1)
ONOO−
H2O2
NO
NO2−
O2•−
NO
g
Cell top
NO2−
NO
H2O2
ONOO−
f (amol s−1)
Time (×10³) (s)
h
O2•−
NO
f (amol s−1)
Time (×10³) (s)
i
P = 0.036
P < 0.001
P < 0.001
P = 0.001
f (amol s−1)
ONOO−
H2O2
NO
NO2−
O2•−
NO

Fig 3

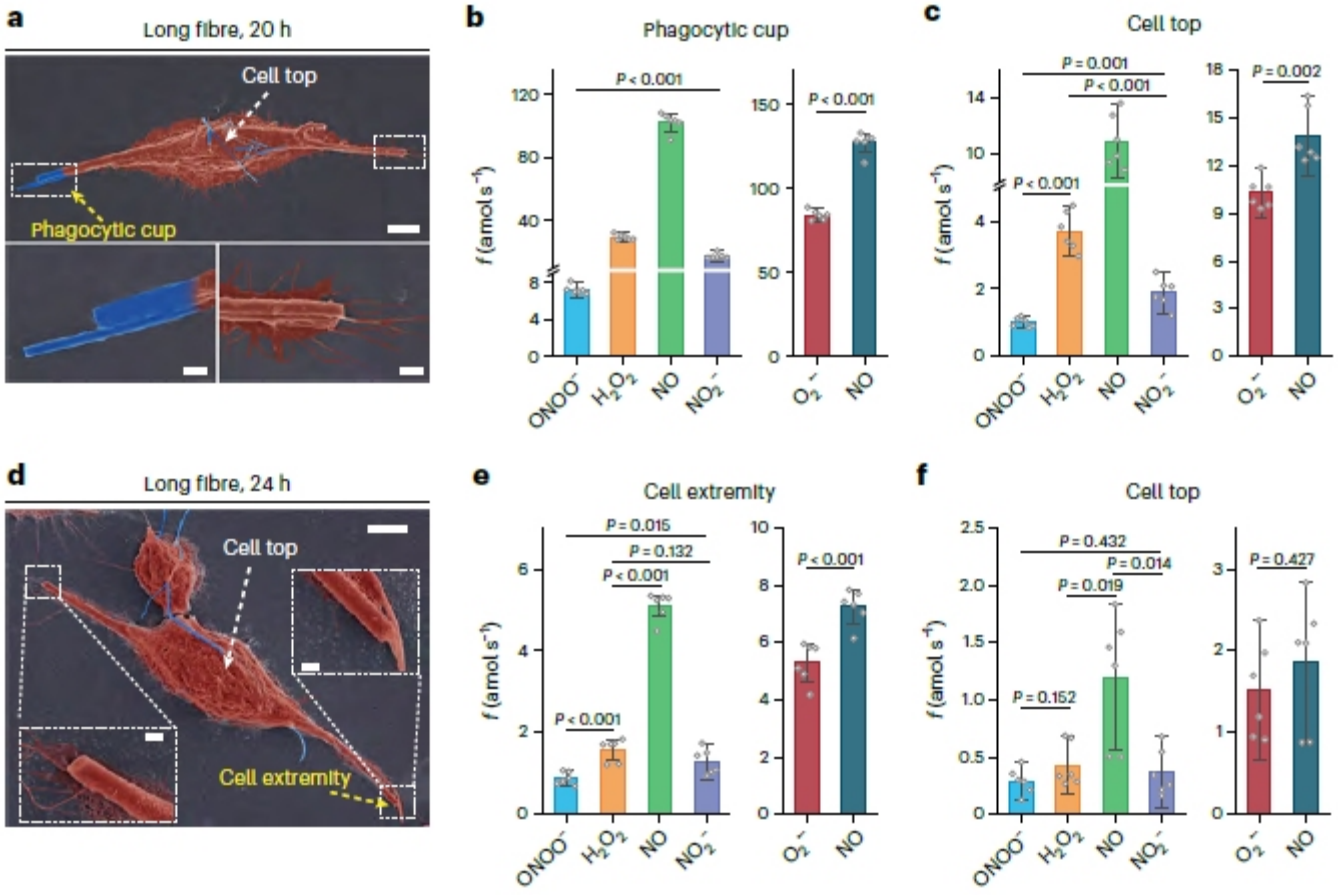
a
Long fibre, 20 h
Cell top
Phagocytic cup
b
Phagocytic cup
P < 0.001
P < 0.001
f (amol s⁻¹)
ONOO⁻
H2O2
NO
NO2⁻
O2⁻
NO
c
Cell top
P = 0.001
P < 0.001
P < 0.001
P = 0.002
d
Long fibre, 24 h
Cell top
Cell extremity
e
Cell extremity
P = 0.015
P = 0.132
P < 0.001
P < 0.001
P < 0.001
f
Cell top
P = 0.432
P = 0.014
P = 0.019
P = 0.152
P = 0.427

Fig 4

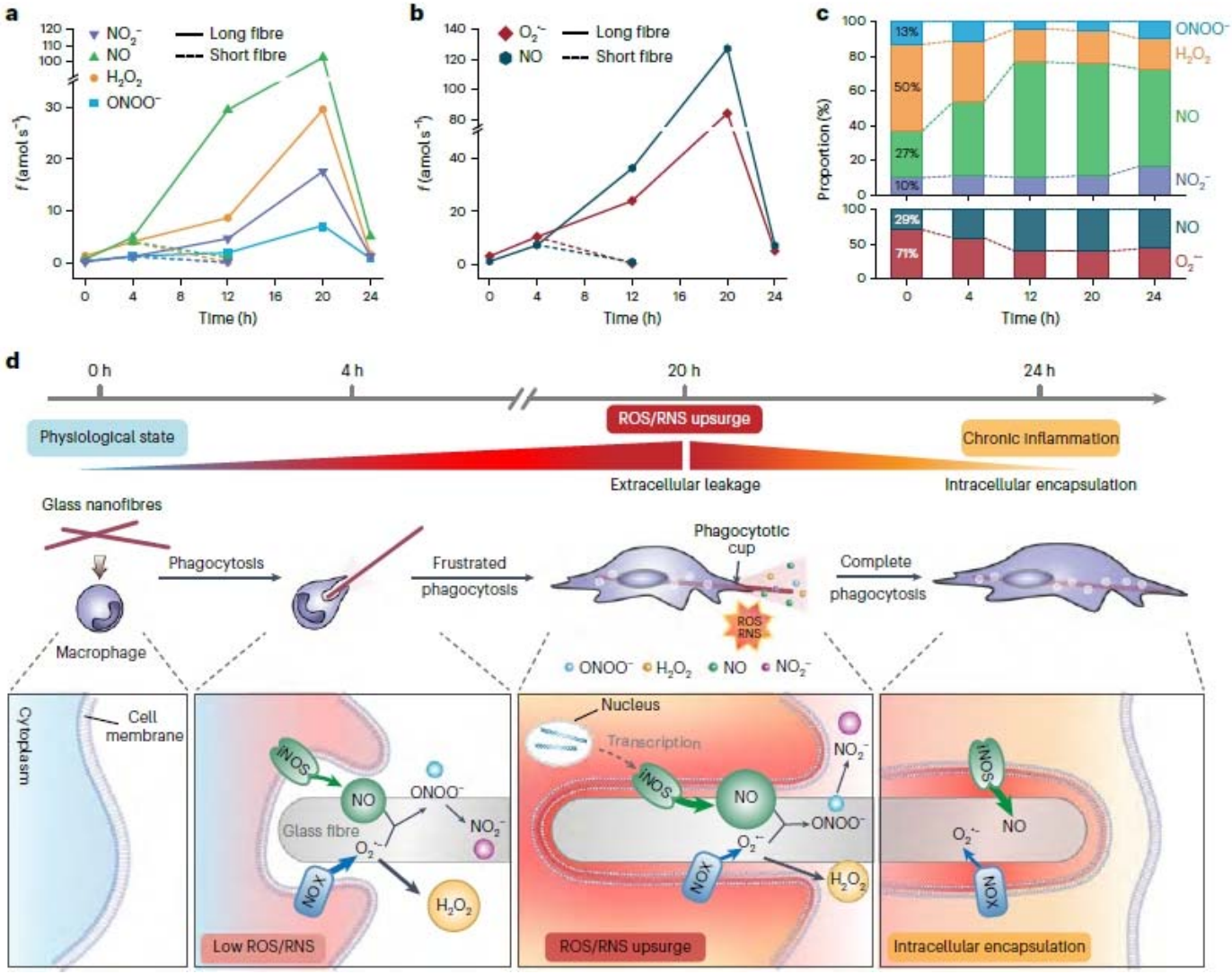
a
NO_2^-
NO
H_2O_2
$ONOO^-$
Long fibre
Short fibre
f (amol s^{-1})
Time (h)
b
$O_2^{\cdot-}$
NO
Long fibre
Short fibre
f (amol s^{-1})
Time (h)
c
Proportion (%)
13%
50%
27%
10%
29%
71%
$ONOO^-$
H_2O_2
NO
NO_2^-
$O_2^{\cdot-}$
Time (h)
d
0 h
4 h
20 h
24 h
Physiological state
ROS/RNS upsurge
Chronic inflammation
Extracellular leakage
Intracellular encapsulation
Glass nanofibres
Phagocytosis
Frustrated phagocytosis
Phagocytotic cup
Complete phagocytosis
ROS RNS
Macrophage
$ONOO^-$ H_2O_2 NO NO_2^-
Cytoplasm
Cell membrane
iNOS
NO
$ONOO^-$
NO_2^-
Glass fibre
$O_2^{\cdot-}$
NOX
H_2O_2
Low ROS/RNS
Nucleus
Transcription
ROS/RNS upsurge
Intracellular encapsulation

Fig 5

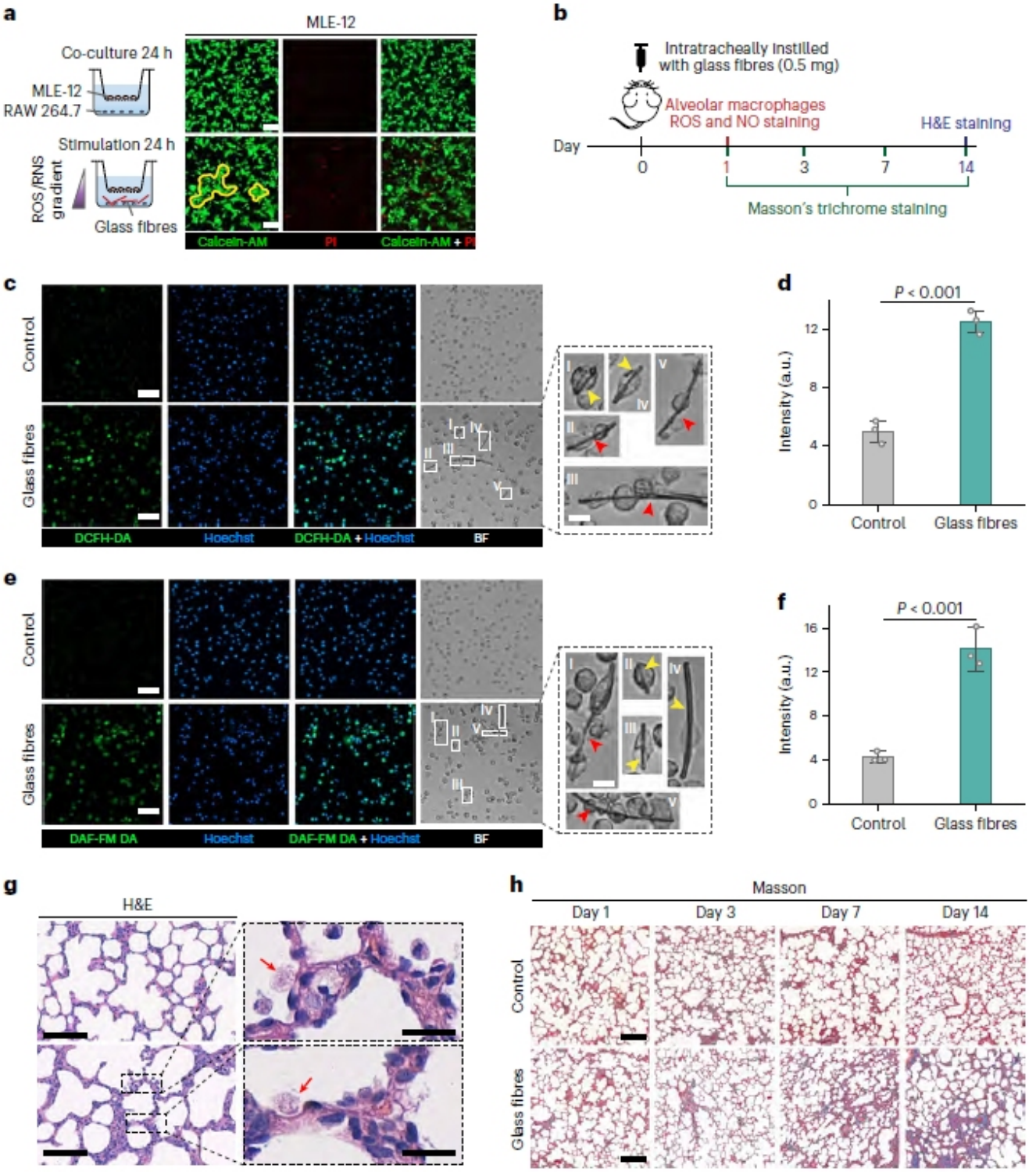
a
MLE-12
Co-culture 24 h
MLE-12
RAW 264.7
Stimulation 24 h
ROS /RNS gradient
Glass fibres
Calcein-AM
PI
Calcein-AM + PI
b
Intratracheally instilled with glass fibres (0.5 mg)
Alveolar macrophages ROS and NO staining
H&E staining
Day
0
1
3
7
14
Masson's trichrome staining
c
Control
Glass fibres
DCFH-DA
Hoechst
DCFH-DA + Hoechst
BF
d
P < 0.001
Intensity (a.u.)
Control
Glass fibres
e
Control
Glass fibres
DAF-FM DA
Hoechst
DAF-FM DA + Hoechst
BF
f
P < 0.001
Intensity (a.u.)
Control
Glass fibres
g
H&E
h
Masson
Day 1
Day 3
Day 7
Day 14
Control
Glass fibres

Fig 6

Methods

Quantitative Characterization of Individual ROS/RNS Fluxes

Each of the four primary ROS/RNS emitted during phagocytosis is oxidizable electrochemically upon application of a specific potential (+150, 550, 650, 800 mV vs. Ag/AgCl) to the SiC@Pt nanowire electrochemical sensors (Extended Data Fig. 3a).[17,19,27,31] In fact, since electrochemical currents are additive, the amperometric currents monitored at each of these four potentials probed sequentially upon using the periodical potential-step progression shown in Extended Data Fig. 3b are given at any time t by:[17]

$$i_{150\,mV}(t) = i_{ONOO^-}(t) + 0.1 i_{H_2O_2}(t) \quad (1)$$

$$i_{550\,mV}(t) = i_{ONOO^-}(t) + i_{H_2O_2}(t) + 0.1 i_{NO}(t) \quad (2)$$

$$i_{650\,mV}(t) = i_{ONOO^-}(t) + i_{H_2O_2}(t) + i_{NO}(t) \quad (3)$$

$$i_{800\,mV}(t) = i_{ONOO^-}(t) + i_{H_2O_2}(t) + i_{NO}(t) + i_{NO_2^-}(t) \quad (4)$$

where $i_{potential}(t)$ is the total current measured at each selected potential at the time t, while $i_{species}(t)$ is the individual limiting plateau current of the named species (Extended Data Fig. 3a) that would be observed at the same time t if this species was alone at the same concentration under the same conditions.[17,19,27,31] In the practice, to eliminate transient capacitive and background currents generated after each potential jump (compare Extended Data Fig. 3c), all $i_{potential}$ values were recorded at the end of 20 s potential steps.[17,29,31] Note in equations (1) or (2) the presence of a 10% fraction of H_2O_2 or NO plateau currents, respectively, due to the incomplete separations of the $ONOO^-$ and H_2O_2 waves (Eqn. 1) or H_2O_2 and NO waves (Eqn. 2) (compare Extended Data Fig. 3a).[17,27,31]

Each individual plateau current value for each species could then be easily extracted every 20 s through solving the linear system of equations in equations (1-4). The time-dependent production rates of each primary ROS/RNS species, $f_{species}(t)$, could be then calculated from the time variations of each individual current, $i_{species}(t)$, according to Faraday's law: $f_{species}(t) = \frac{i_{species}(t)}{z_{species}F}$, where $F = 96500$ C is the Faraday constant and $z_{species}$ is the electron stoichiometry of the species electrochemical oxidation at black-Pt electrodes ($z_{H_2O_2} = z_{NO_2^-} = 2$; $z_{ONOO^-} = z_{NO} = 1$).[17,27,31]

A cylindrical nanoelectrode of radius r_{el} is able to probe only the concentration of electroactive species present inside a coaxial cylindrical solution domain of radius δ given by:[47-50]

$$\delta = r_{el} \ln(2\sqrt{D\Delta t}/r_{el}) \quad (5)$$

where D is the diffusion coefficient of the species (i.e., ca. 2×10^{-9} $m^2 s^{-1}$ for ROS/RNS)[49] and Δt= 20 s is the duration between two measurements (Extended Data Fig. 3b), so that $\delta \approx$ 1.5 µm for the SiC@Pt nanowire sensors used in this work according to the potential-step procedure described in the previous section. In other words, the SiC@Pt nanowire sensors used here act as electrochemical microscopes with a spatial resolution of ca. 1.5 µm and a temporal resolution of 20 s. This unique property makes it possible to study the intensities and chemical nature of ROS/RNS fluxes emitted by macrophages at specific locations on their bodies surfaces

and at different stages (0, 4, 12, 20 and 24 h) of their frustrated phagocytosis of glass nanofibers (as sketched in Fig. 1a on the right).

Fabrication of SiC@Pt NW Sensors

Mechanical procedures of SiC@Pt NW sensors fabrication were identical to those described in refs.[17] (NW = NanoWire). Briefly, SiC nanowires (ca. 200 nm diameter; Nanjing/Jiangsu XFNANO Materials Tech) self-coated with high-density Pt nanoparticles (SiC@Pt NWs) obtained by reducing H_2PtCl_6 with HCOOH. The ensuing SiC@Pt NWs were dispersed in 20 mL ultrapure water and added dropwise to the center of a glass sheet and gently heated to evaporate water. Then the glass sheet was cut into two parts to allow for a partial protrusion of NWs over the glass slide edges. Next, using microforges manipulators, each SiC@Pt NW was carefully inserted into a prepared glass micropipette holder filled with liquid metal and wax to fabricate one SiC@Pt NW sensor with the protruding length of 5 µm.

Preparation and Characterization of Glass Nanofiber

Glass nanofibers utilized in the experiments were extracted from quartz filter membranes (Munktell Filtrak™ Grade MK5) whose structure involves glass fibers with moderately dispersed dimensions. Filters were firstly combusted at 450°C during 6 h to remove organic matter and microorganisms, and the individual glass fibers were separated from the crushed filter membranes (40 mg) through sonication in 20 mL water at 25 °C during 60 min at a frequency of 90 Hz. The long fibers were left to settle under gravity during 20 min, after which the resulting supernatant was decanted. The sedimented fraction was filtered three times through a 70 µm mesh (ChuangWei, China) to separate the residual long fibers.[6,8] Conversely, the short fibers were collected from the filtrate and filtered three times through a 10 µm mesh (ChuangWei, China).[6,8] This allowed to recover glass fibers with lengths smaller than 10 µm. These were freeze-dried during 24 h and diluted in a culture medium or buffer to obtain a 2 mg/mL stock solution which was then sonicated (50 Hz) for 30 s at 25 °C to disperse the fibers while avoiding fiber fragmentation under aggressive sonication. The stock solutions were shaken to redisperse the fibers before each experiment with cells or for intratracheal administration. Glass nanofibers were imaged with scanning electron microscopy (Zeiss Sigma) equipped with energy-dispersive X-ray spectroscopy spectrometer (X-MaxN) to analyze fiber diameter, length, aspect ratio and elemental composition.

10 mg crushed filter membranes were dispersed into absolute ethanol (15 mL) followed by 200 µL FITC/APTES conjugate addition into it.[51,52] The mixed solution was stirred magnetically at 25°C for 24 h.[51,52] Finally, the FITC-labelled glass nanofibers were extracted according to the above procedure and washed 3 times with ultrapure water. All the above operations were carried out in the dark to prevent dye bleaching.

Cells Experiments

RAW 264.7 cells (Procell Life Science & Technology) were cultured in DMEM medium supplemented with 10% fetal bovine serum, 1% horse serum, and 1% penicillin/ /streptomycin at 37 °C under 5% CO_2 atmosphere. Before performing any experiment, the RAW 264.7 cells were seeded on small cell culture dishes (diameter 35 mm). After cell adhesion, 50 µg/mL glass nanofibers were added to stimulate macrophages

activation from M0 type to polarized type. Before the electrochemical experiments, the tested cells were transferred into a new cell culture medium.

The lung epithelial cells MLE-12 (Bluefbio Life Science & Technology) were seeded into the upper chamber of the transwell (0.4 μm pore size; Biofil) and incubated for 12 h to allow their proliferation into a confluent monolayer in DMEM with 10% FBS and penicillin/streptomycin. The upper chambers containing these cells were placed into the wells of twelve-well plates whose down chambers contained with or without adherent RAW 264.7 macrophages treated in parallel containing DMEM or 50 μg/mL glass nanofibers (see sketches in Extended Data Fig. 10a). Co-culture cells were cultured in a standard humidified incubator at 37 °C in a 5% CO_2 atmosphere for 24 h.

in vivo Experiments

Rats (Sprague-Dawley/males, 8 weeks old, ~300 g body weight) were purchased from Hunan STJ laboratory animal Co., Ltd.

The institutional review board (Approval No. HLK-20220403-001) confirms that the animal experiment design in the application is sensible, conforms to the "3R" principle of laboratory animals, and strictly complies with the "Guidelines for the Use and Management of Laboratory Animals" issued by the National Institutes of Health (NIH) of the USA and the relevant regulations of the "Implementation Rules for the Management of Medical Laboratory Animals" issued by the National Health and Family Planning Commission of China. The investigators are qualified to undertake the proposed project. All materials meet the requirements of the "Ethical Review System for Laboratory Animal Welfare of the Wuhan Myhalic Biotechnology Co., Ltd."

The experimental design and duration of glass fiber exposure shown in Fig. 6b illustrated our evaluation of alveolar macrophages' status and pulmonary lesions after pulmonary exposure to glass fibers. In summary, rats were randomized into two groups of 20 rats (control and test groups). The rats were dispensed a single exposure of PBS (control group) or PBS-suspended glass nanofibers (2 mg/rat, tested group) using intratracheal instillation. After 1 day following the exposure, some rats (control PBS n=4; glass fibers, n=4) were anesthetized with 3% sodium pentobarbital intraperitoneally and administered a bronchoalveolar lavage (BAL) fluid to isolate alveolar macrophages. Animals in each of the other groups (controls n=4; glass fibers, n= 4) were anesthetized with pentobarbital and killed by exsanguination at 1, 3, 7, and 14 days of exposure, respectively, for lung tissue collection.

The whole lung was washed three times with 3 mL PBS solution per rat. Collected bronchoalveolar lavage (BAL) fluid was centrifuged (400 G, 5 min, 4 °C) and the sedimented pellet was then suspended and incubated in red blood cell (RBC) lysis buffer for 5 min without light. The suspension was centrifuged (400 G, 5 min, 4 °C) twice and then the pellet was suspended in the complete 1640 medium for the follow-up experiments.

The surgically resected lung was fixed overnight in a neutral 10% formalin buffer and then transferred to 70% ethanol and embedded in paraffin. The lung sections (4 mm) were processed for histopathology with hematoxylin and eosin stain and Masson's trichrome stain.

Imaging

The RAW 264.7 macrophages and MLE-12 cells were incubated with 5 μM calcein-AM (tetraacetoxymethylester; Sigma-Aldrich) and 3μg/mL PI (propidium iodide; Sigma-Aldrich) for 20 min, and residual dyes were washed off with PBS solution for 3 times. Bright-field and fluorescence microphotographs (AxioObserver Z1, Zeiss) were then recorded with an inverted fluorescent microscope as soon as possible.

M0 and polarized RAW 264.7 cells (after 0, 4, 12, 20 and 24 h of frustrated phagocytosis of glass nanofibers) were fixed with 4% paraformaldehyde for 10 minutes, permeabilized with 0.1% Triton X-100 for 15 minutes. Fixed and permeated M0 and polarized RAW 264.7 cells were then incubated with 555-phalloidin (dilution 1:40; UElandy) and Hoechst 33342 (dilution 1:1000; Sigma-Aldrich) for 30 min and washed 3 times with PBS. Confocal microphotographs (LSM900, Zeiss) were recorded as soon as possible.

The videos of macrophage behavior were recorded with a confocal microscope (LSM900, Zeiss) using 20× objective lens equipped with an incubation chamber, heated stage and CO_2 mixer (PECON, Zeiss). RAW 264.7 macrophages were seeded on a small cell culture dish (diameter 35 mm) and incubated for 30 min to allow their adhesion to the dish bottom. After changing the DMEM medium with or without 50 μg/mL glass nanofibers, the cell culture dish was placed in the incubation chamber and bright-field photographs were recorded every 3 min. To visualize the dynamic processes of cell membranes in frustrated phagocytosis, adherent macrophages were incubated with 25 μM CellTracker Orange (Thermo Fisher) for 45 min and washed 3 times with PBS. Subsequently, cells were treated with DMEM medium with or without 50 μg/mL FITC-labelled glass nanofibers and fluorescent images were recorded every 1 h.

M0 and polarized RAW 264.7 cells (after 0, 4, 12, 20 and 24 h of frustrated phagocytosis of glass nanofibers) were fixed with 4% paraformaldehyde for 10 minutes, permeabilized with 0.1% Triton X-100 for 15 minutes, and blocked with 1.5% goat serum for 60 minutes at room temperature. The cells were labeled with iNOS monoclonal fluorescent antibody (Alexa Fluor 488) (dilution 1:25; Thermo Fisher) at 4℃ overnight. Nuclei and F-actin were stained with Hoechst 33342 (dilution 1:1000) and phalloidin (dilution1:40) respectively for 30 min and washed with PBS for 3 times. Confocal microphotographs were then recorded as soon as possible.

The alveolar macrophages from bronchoalveolar lavage fluid were fixed with 4% paraformaldehyde during 10 minutes, permeabilized with 0.1% Triton X-100 for 15 minutes, and blocked with 1.5% goat serum for 60 minutes at room temperature. 20 μg/mL of anti-mouse Siglec F (Thermo Fisher) was incubated with cells at 4℃ overnight. Goat anti-rat IgG Alexa Fluor 488 (dilution 1:200; Thermo Fisher), Hoechst 33342 (dilution 1:1000) and 555-phalloidin (dilution1:40) were incubated with cells for 60 min at room temperature and washed with PBS for 3 times. Confocal microphotographs were then recorded as soon as possible.

The alveolar macrophages from bronchoalveolar lavage fluid were incubated with 5 μM DAF-FM DA (3-amino,4-aminomethyl-2',7'-difluorescein diacetate; Beyotime Biotechnology) solution or 5 μM DCFH-DA (2',7'-dichlorodihydrofluorescein diacetate; Beyotime Biotechnology) solution and 5 μg/mL Hoechst for 25 min and washed 3 times with PBS. Bright-field and confocal microphotographs were then recorded with a confocal microscope as soon as possible.

Flow Cytometry

Cells (from Raw 264.7 macrophages after 24 h of frustrated phagocytosis or BAL fluid) were stained with appropriate antibody cocktails at 4 °C following flow cytometry antibodies were used: F4/80 (BM8), CD86 (GL1), iNOS (CXNFT), CD206 (MR6F3), arginase 1 (A1exF5), CD86 (B7-2) from eBioscience or Invitrogen. Samples were run using a flow cytometer (NovoCyte, ACEA) and analyzed with FlowJo software (v10.8.1 version). Gating strategies are provided in the Extended Data Figure 1.

Cytokine and Cytotoxicity Detection

Raw 264.7 macrophages were seeded in 24-well plates (2.5×10^4 cells/cm^2) for cytokine and cytotoxicity detection. After 24 h of cell-fiber incubation, supernatants were harvested for TNF-α (Multi Sciences), IL-1α (NeoBioscience), and PGE-2 (Multi Sciences) and assayed with a multimode dispenser (Epoch, BioTeK) according to the manufacturer's protocol for ELISA assays. Supernatants were also used to determine cytotoxicity by measuring lactate dehydrogenase (LDH) activity (Beyotime).

Amperometric Data Acquisition and Analysis

All amperometric measurements involving living cells were performed inside a well-grounded Faraday cage under an inverted microscope (AxioObserver Z1, Zeiss) control equipped with a 40× or 100× objective lens. Single SiC@Pt NW sensors tips were precisely controlled by a micromanipulator (TransferMan 4r, Eppendorf) to be in slight contact (vz., less than 500 nm) with the detection points without interfering with the release phenomena. The amperometric traces were recorded with a 2-electrode electrochemical system using a patch-clamp amplifier (EPC-10 HEKA Electronics, Germany) at a series of selected potentials (150, 550, 650, and 800 mV vs. Ag/AgCl). Amperometric traces were sampled at 1 Hz.

In a different series of experiments SiC@Pt NW sensors were scanned close to the macrophages' membrane surface following the partially captured glass fibers axis with 2 µm steps (see the bright-field images sequences in Extended Data Fig. 6a, Extended Data Fig. 7a and Extended Data Fig. 8a). This was performed to display the relationship between the positions on the cells surface and the global ROS/RNS-related current intensities (graphs in Extended Data Fig. 6, Extended Data Fig. 7a-b and Extended Data Fig. 8a-b). Indeed, at each position, currents were recorded during 20 s at +800 mV vs. Ag/AgCl and averaged to measure the mean amount of total ROS/RNS released at this point. This method was used in particular to determine the location of the "phagocytic cups".

The protocol of quadruple potential chronoamperometric sequences was performed as reported in refs.[29,33] after slightly modifying some details as indicated below. A sequence of potential steps (+150, +550, +650 and +800 mV) with step durations of 20 s each were applied to the SiC@Pt NW sensors (Fig. 2b). The currents were sampled at the end of each 20 s long potential step (Extended Data Fig. 3c) in order to minimize the charging currents contributions. A pre/postcalibration was performed by positioning the electrode far away from the cell and cycling its potential for 30 min before and after each experiment. Any drift in the baseline was then subtracted from the recorded response to yield the final chronoamperograms.

Raw amperometric data were gathered with the "Pulse" software and analyzed by the "Origin 2021

Graphing &Analysis" software.

The ROS/RNS release fluxes were recorded over 1.5 h with the nanoelectrode placed on the detection position after 4, 12, 20 and 24 h of phagocytosis by an individual macrophage. After subtraction of the baseline (current intensity values for M0 cells), 70 data points were recorded for each four primary ROS/RNS and averaged into a mean value of ROS/RNS leakage from an individual cell. The error (standard error of the mean, SEM) was taken as the standard deviation of the mean release values for 6 cells.

Statistics and Reproducibility

For each group of amperometric analysis, a minimum of 6 macrophage replicates were analyzed. All cell experiments were conducted using cells derived from the same passage or the same rats' group, and the cells' suspension was cultured in 5-6 wells of the same plate. After subjecting each group to the same treatment, 3 wells were selected randomly for testing and data analysis. SEM imaging, fluorescent staining, immunofluorescent staining, cell video, flow cytometry and detection of cytokine and cytotoxicity were repeated at least 3 times. For data with multiple groups, the statistically significant differences were assessed using one-way ANOVA analyzed with IMB SPSS Statistic (R26.0.0.0 version). The sample sizes (biological replicates), specific statistical tests, error bars (SD and SEM) of mean values, and P values of our statistical analyses are detailed in each figure legend.

Figures Extended Data

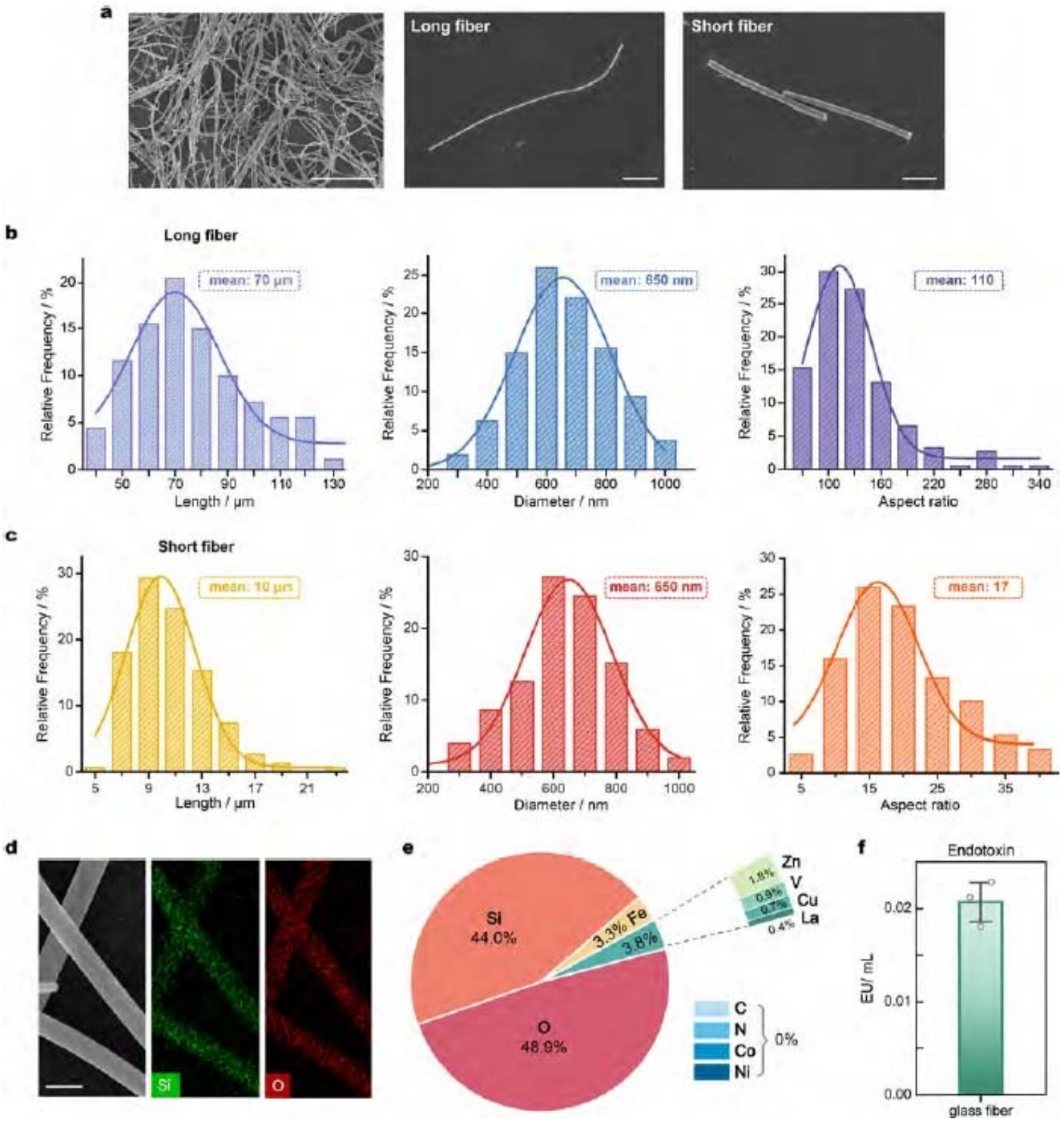

Fig Extended data 1

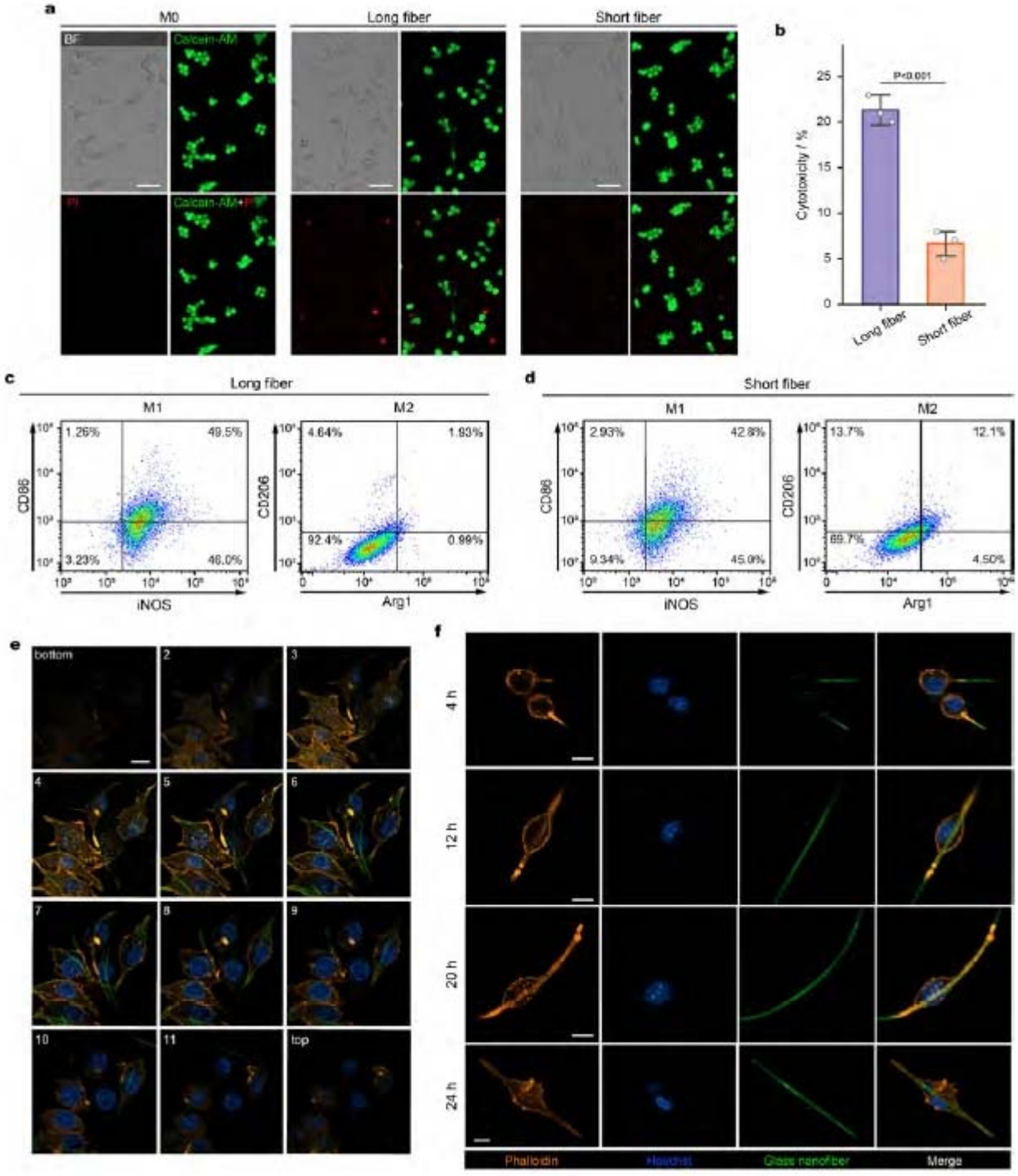

Fig Extended data 2

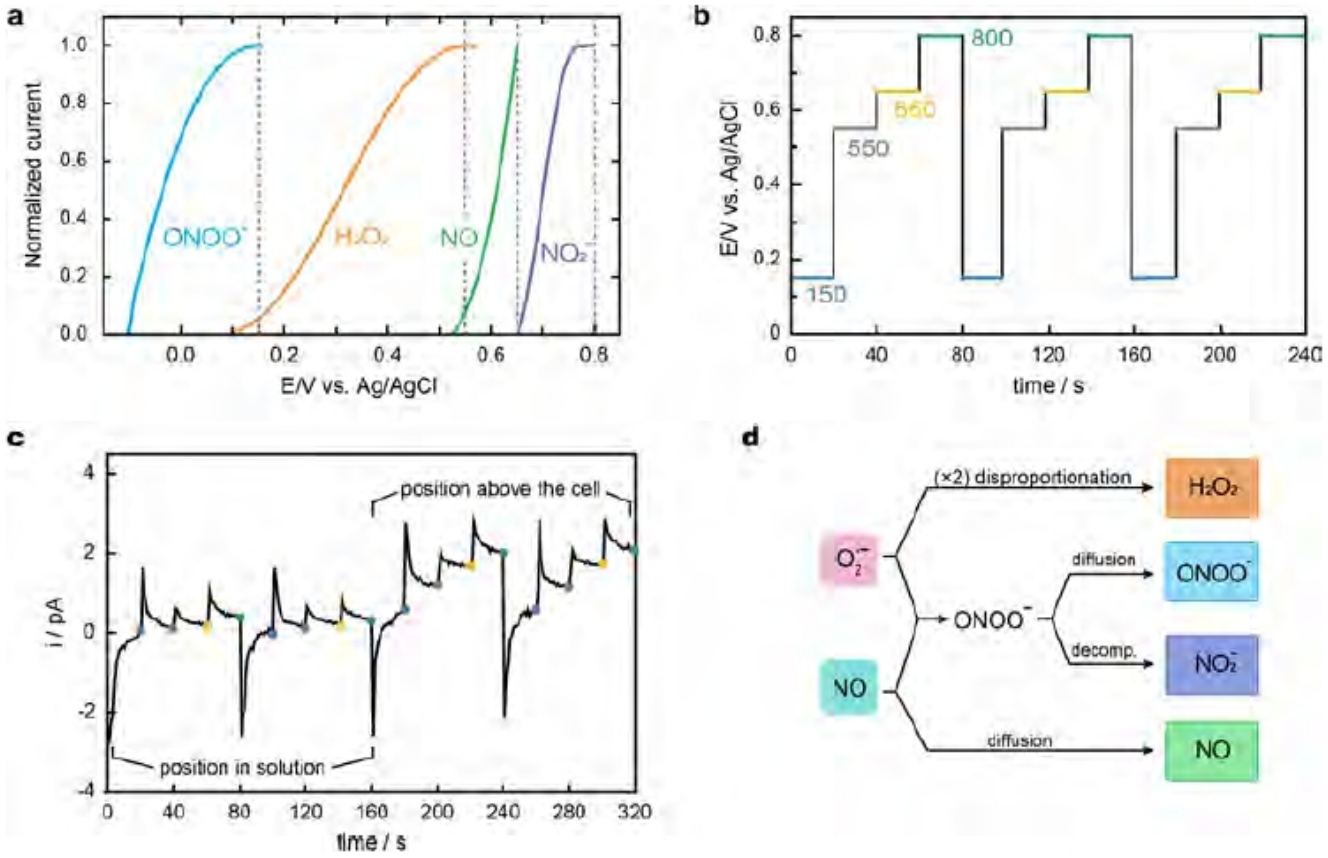

Fig Extended data 3

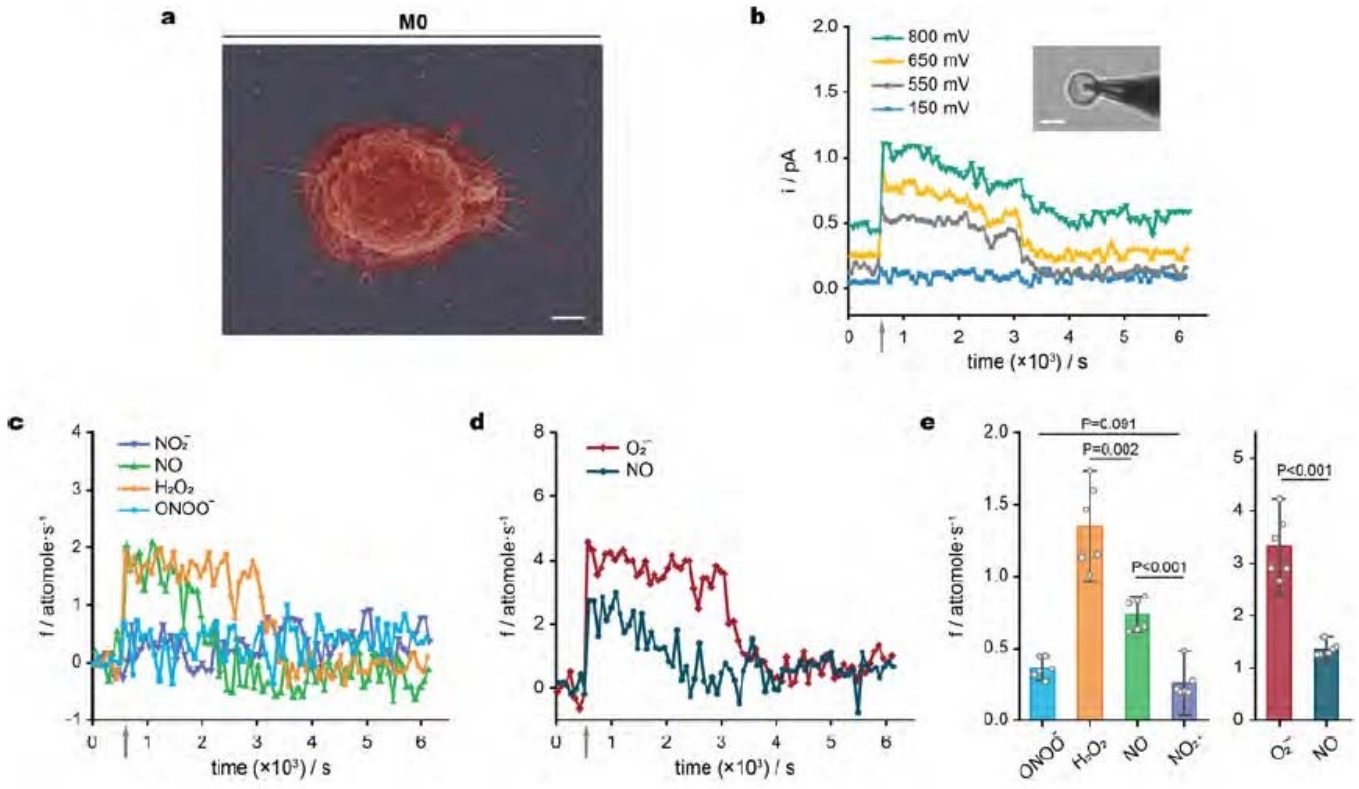

Fig Extended data 4

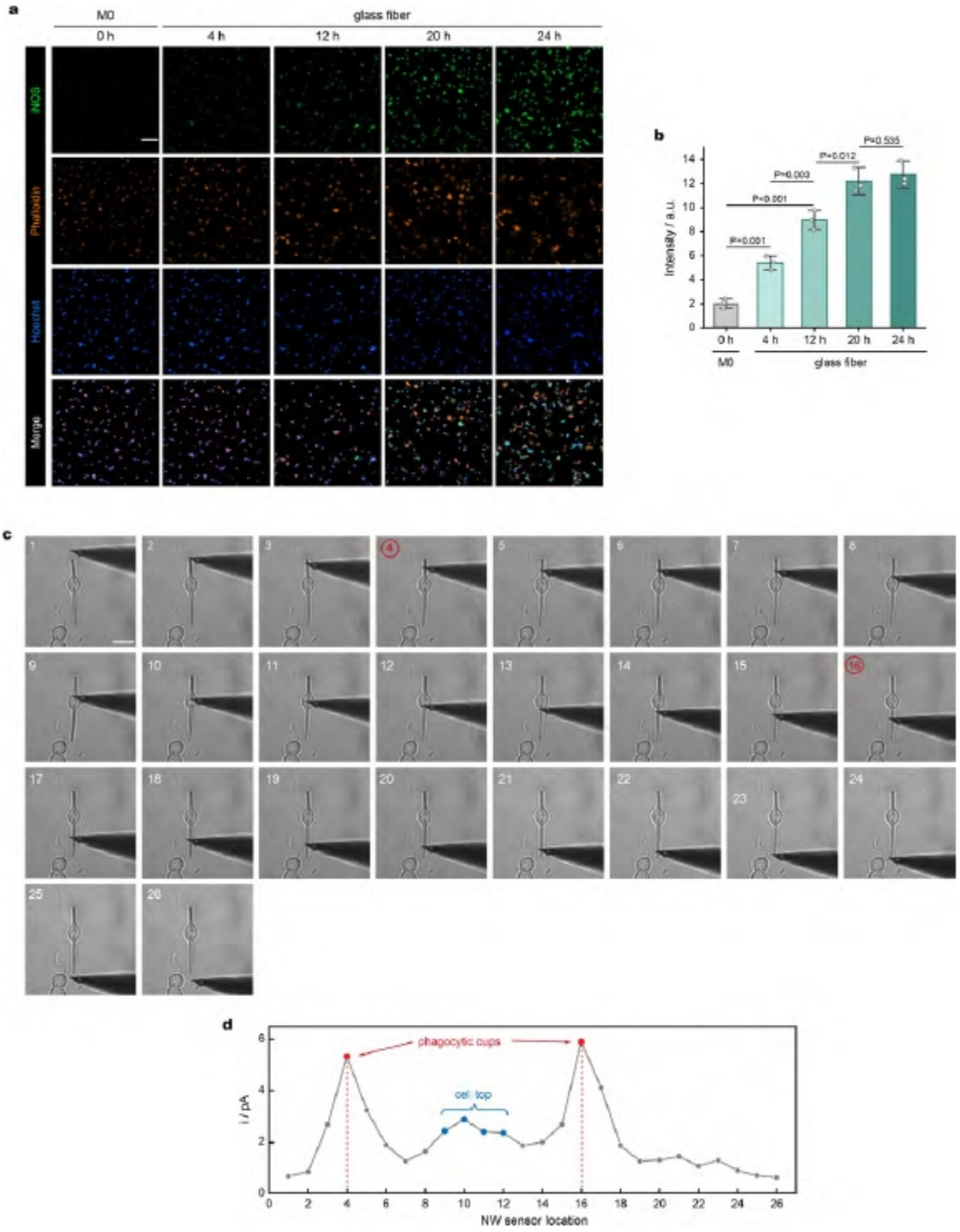

Fig Extended data 5

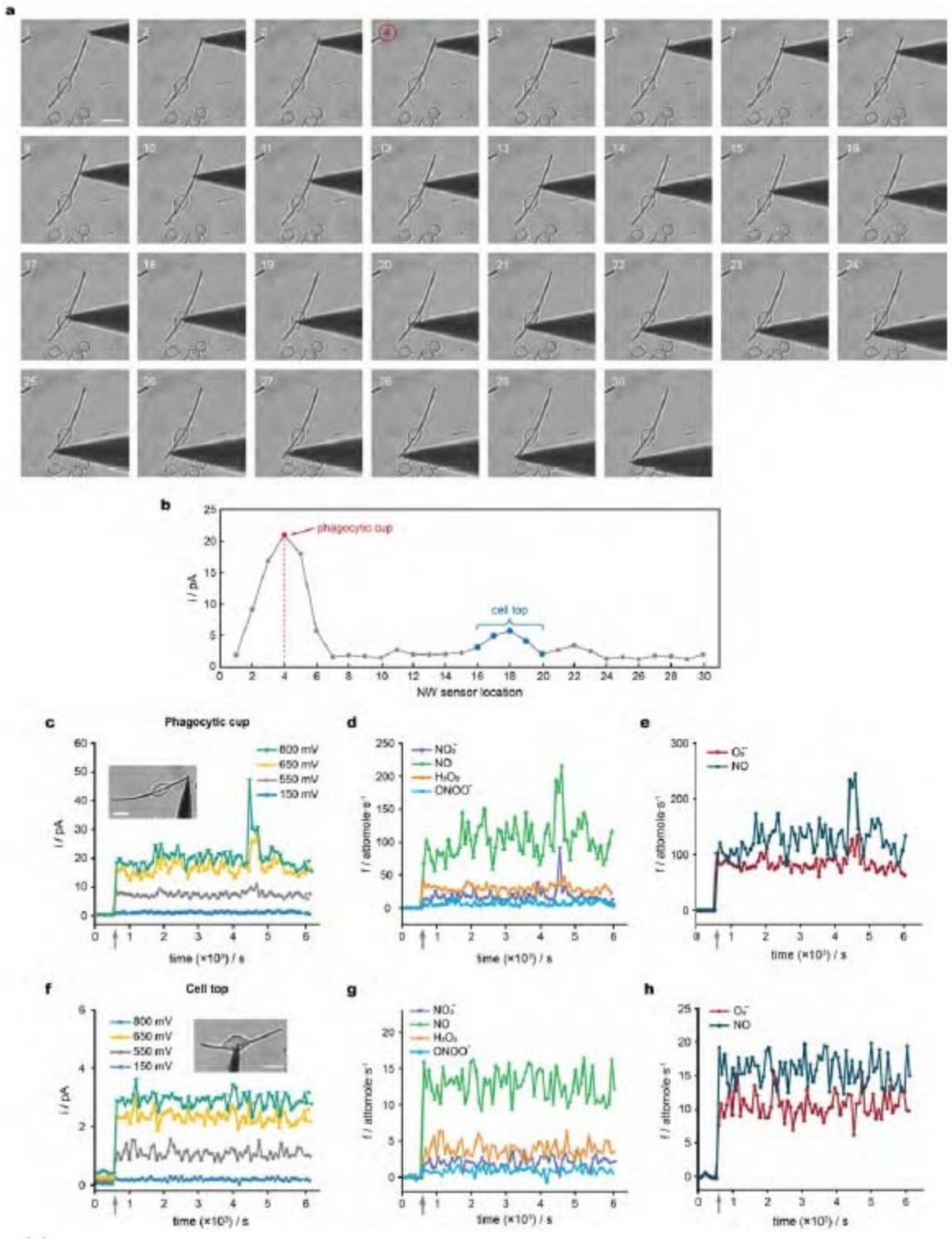

Fig Extended data 6

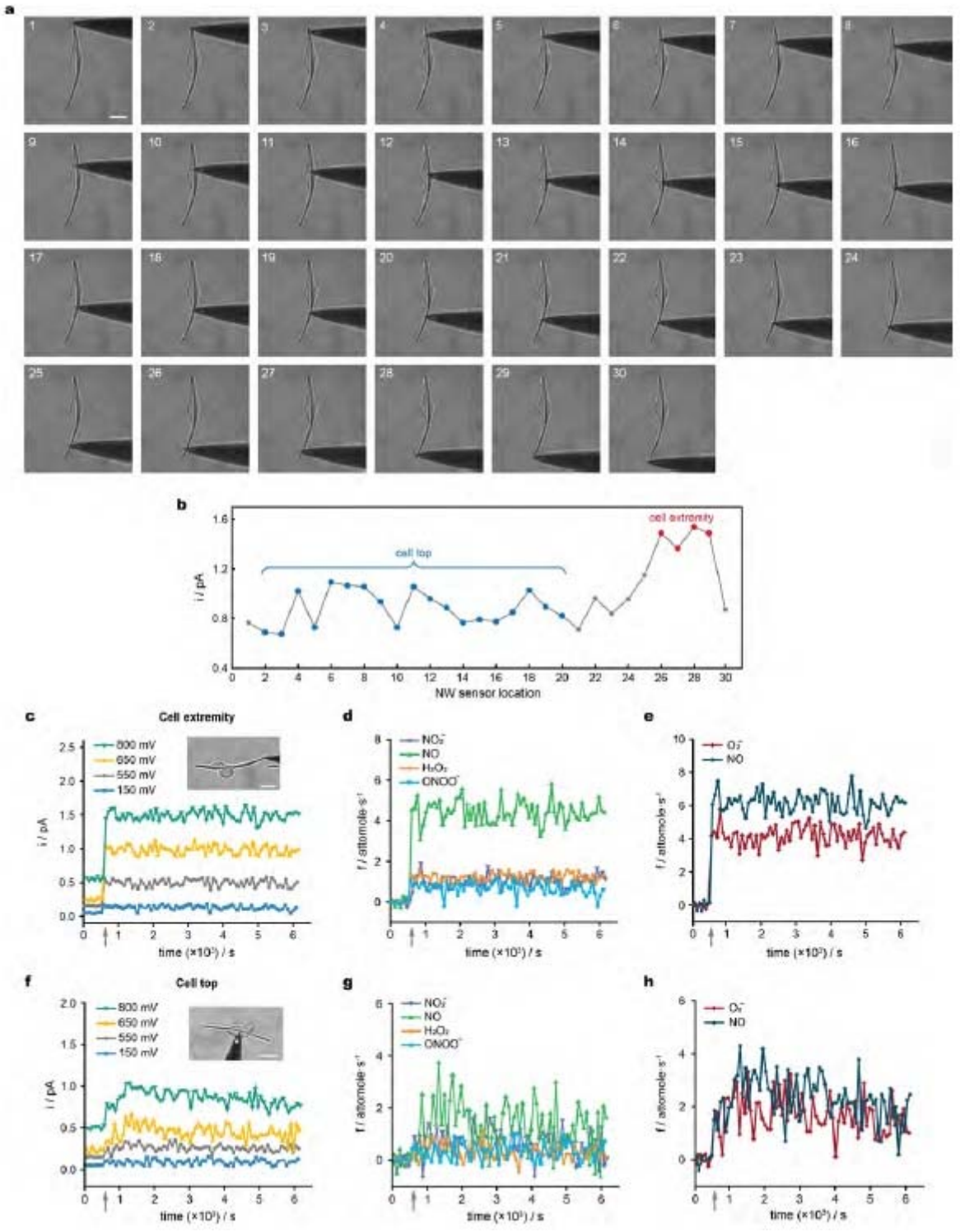

Fig Extended data 7

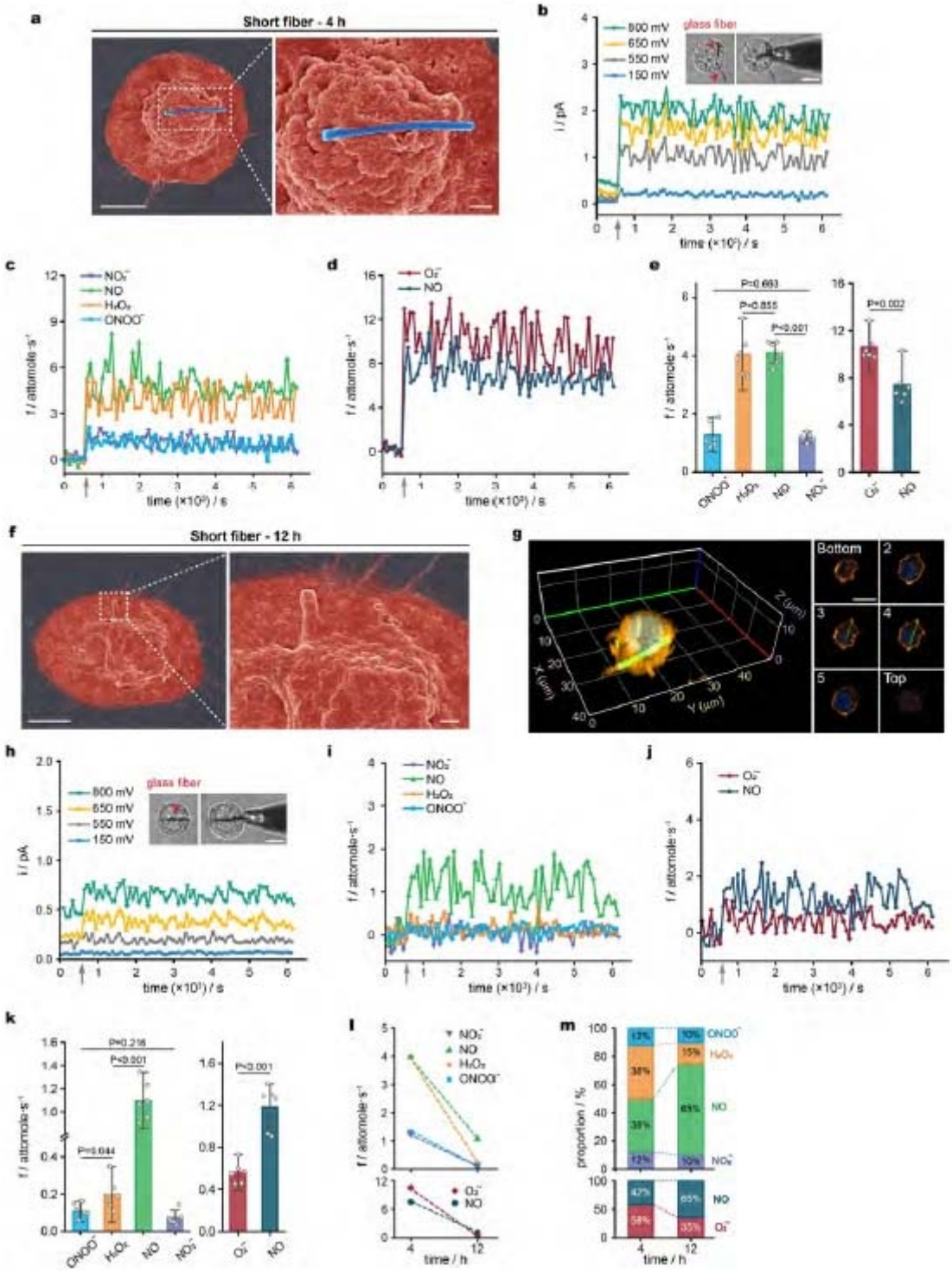

Fig Extended data 8

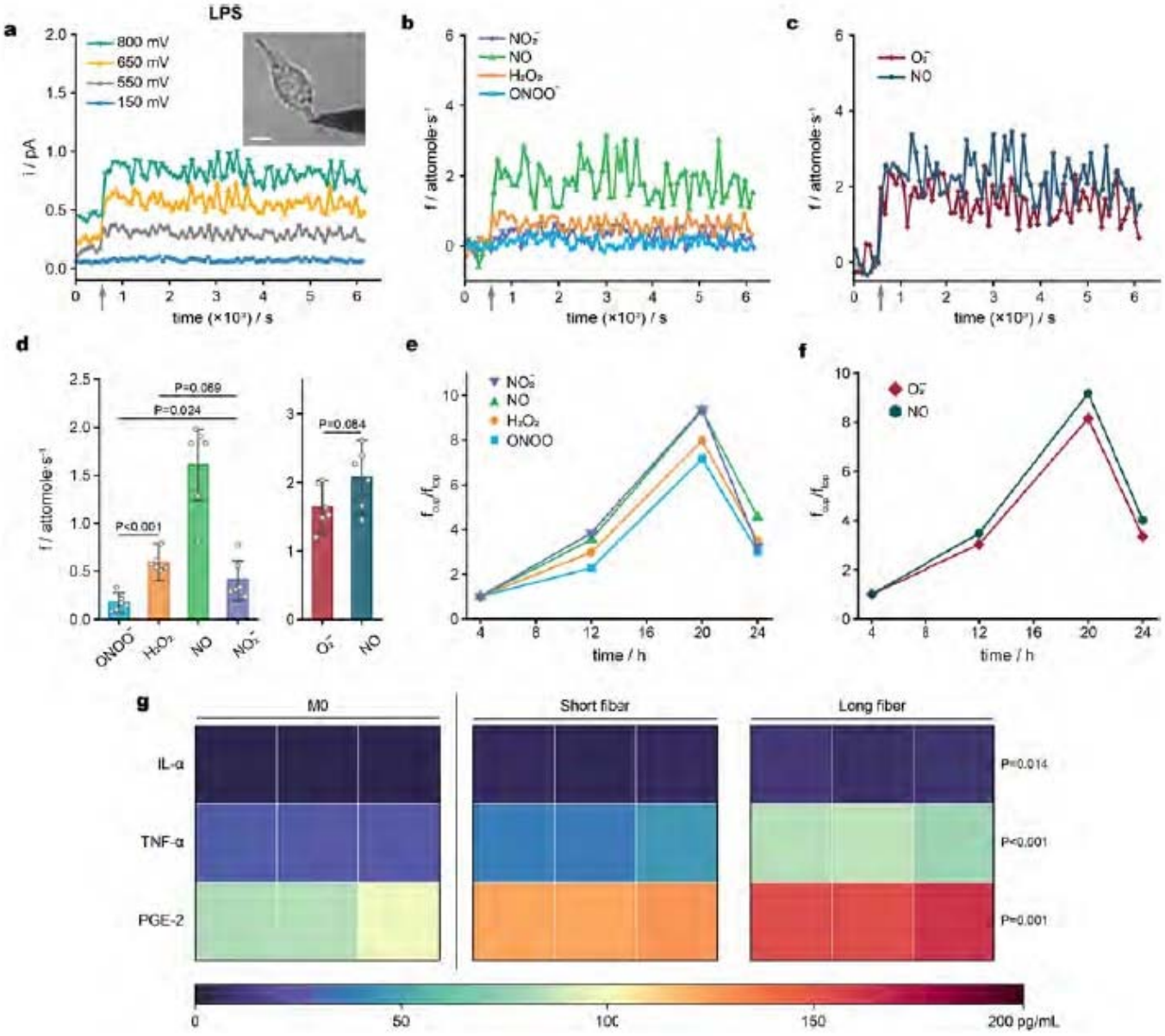

Fig Extended data 9

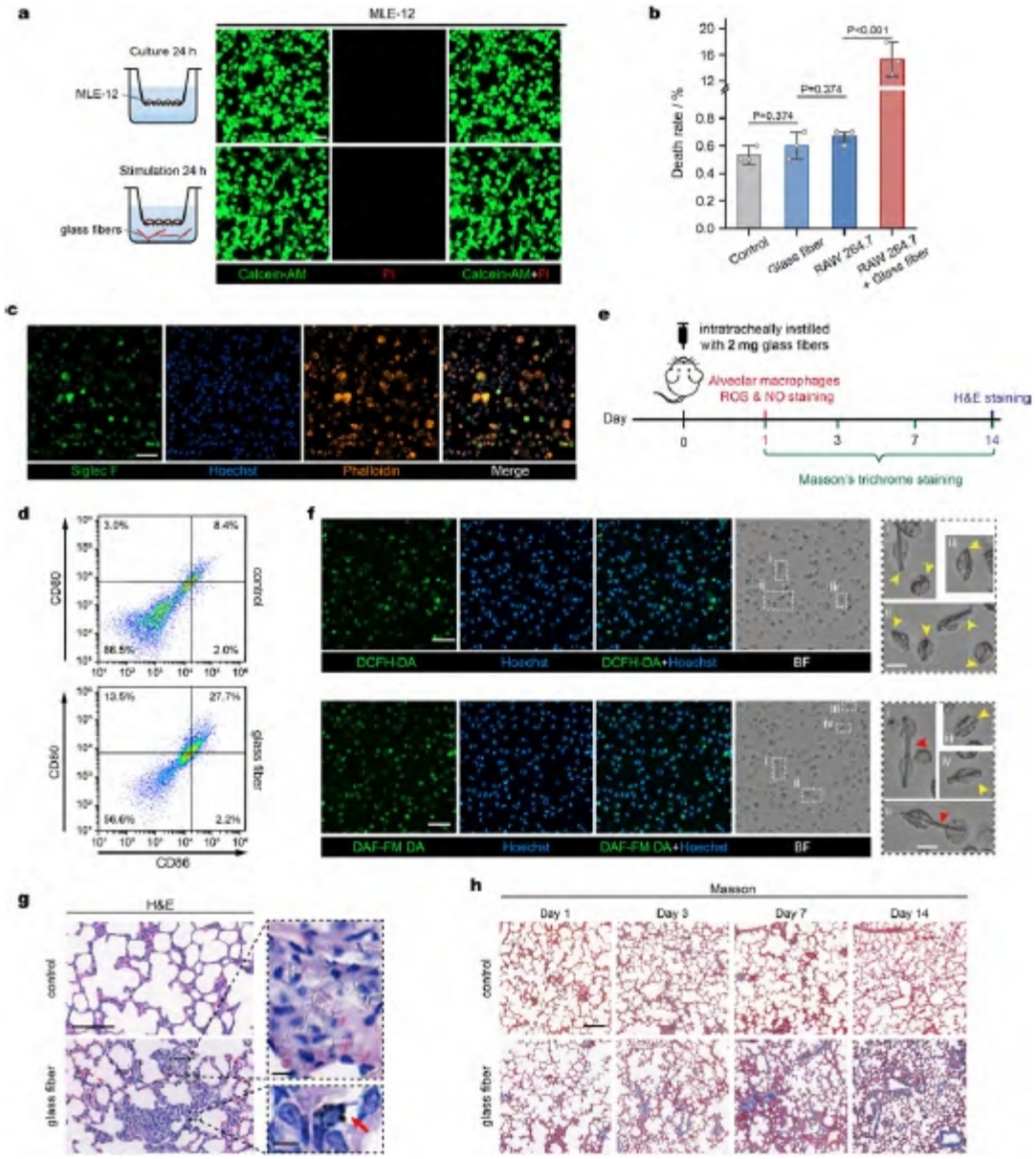

Fig Extended data 10